Green Chemistry

ROYAL SOCIETY OF CHEMISTRY

CRITICAL REVIEW

View Article Online
View Journal | View Issue

Cite this: *Green Chem.*, 2025, **27**, 11705

Green solvents in membrane separation: progress, challenges, and future perspectives for sustainable industrial applications

Boon Kee Voon,†[a] Yen Juin Yap†[a] and Wai Fen Yong *[a,b,c]

Green chemistry and engineering play a vital role in sustainable separation and technology developments. Over the past decade, significant progress has been made in applying green solvents to separation processes, with a focus on reducing the reliance on conventional toxic solvents such as *N*-methyl-2-pyrrolidone (NMP), *N*,*N*-dimethylformamide (DMF), and *N*,*N*-dimethylacetamide (DMAc). Green solvents offer a promising alternative due to their biodegradability, low environmental impact, and minimal health hazards. Nevertheless, most existing studies focus on individual solvents or specific applications, leaving gaps in understanding regarding solvent–polymer compatibility, scalability, and trade-offs between sustainability and separation efficiency, particularly for liquid and gas separations in membrane technology. This review addresses these gaps by categorizing recent advancements in the use of green solvents for membrane fabrication over the past decade. The solvents are grouped into the categories esters, polar aprotic, dipolar aprotic, polar protic, non-polar aprotic, organic salts, and oils. These green solvents include γ-valerolactone (GVL), Cyrene™, Tamisolve® NxG, Rhodiasolv® PolarClean, ionic liquids (ILs), deep eutectic solvents (DESs), and plant-derived oils. This review also evaluates the interactions between these solvents and commonly used polymers using the Hansen solubility parameter (HSP), alongside the CO_2 capture and water purification performance of the resulting membranes. Additionally, current applications of artificial intelligence (AI) tools in solvent selection are discussed, highlighting their potential to predict polymer–solvent compatibility and optimize membrane fabrication formulations. By summarizing recent advancements, evaluating industrial applicability, and identifying unresolved challenges, this review provides a roadmap for the adoption of green solvents in next-generation membrane technologies, urging researchers and industry stakeholders to accelerate the transition toward sustainable solvent-based processes.

Received 22nd June 2025,
Accepted 19th August 2025

DOI: 10.1039/d5gc03161c

rsc.li/greenchem

Green foundation

1. This review highlights the classification of green solvents used in membrane fabrication for gas and liquid separation applications. Recently developed green solvents are discussed, with a focus on solvent–polymer compatibility assessed using the Hansen solubility parameter (HSP) model. Artificial intelligence tools are also explored to aid solvent selection.
2. As an emerging research area, green solvents offer reduced environmental impact and are increasingly important for industries such as water treatment and carbon capture. The review evaluates various types of green solvents and their influence on membrane performance.
3. Key future challenges include scalability and economic feasibility. By integrating HSP analysis, solvent classification, and AI-based selection methods, this review provides valuable insights to support the wider adoption of green solvents. These strategies aim to optimize membrane compatibility and efficiency, contributing to the advancement of sustainable separation technologies.

1. Introduction

Rewinding to the mid-18th century, the onset of industrialization marked a significant technological breakthrough that propelled the global economy to new heights.[1] Environmental issues such as carbon dioxide (CO_2) emissions, greenhouse gases, and water pollution have garnered significant attention. Researchers are now toiling in unremitting efforts to address

[a]*Centre of Excellence for Green and Advanced Technologies in Efficient Separations (GATES), School of Energy and Chemical Engineering, Xiamen University Malaysia, Jalan Sunsuria, Bandar Sunsuria, 43900 Sepang, Selangor, Malaysia. E-mail: waifen.yong@xmu.edu*
[b]*State Key Laboratory of Physical Chemistry of Solid Surfaces, College of Chemistry and Chemical Engineering, Xiamen University, Xiamen 361005, China*
[c]*Gulei Innovation Institute, Xiamen University, Zhangzhou 363200, China*
†Co-first authors.

these challenges and develop solutions that protect nature without compromising economic growth.[2] Additionally, today's firms, including governments, shareholders, and investors, increasingly prioritize sustainability and environmental protection in their investment decisions. They are more inclined to make 'green investments' to ensure resource efficiency.[3] This shift has driven the advancement of green technologies and demanded greater efforts in green development.

Membrane technology has gained recognition as a green approach because of its environmental friendliness, ease of operation, high energy efficiency, compact footprint, and cost-effectiveness.[4,5] Membrane technology has seen increasing application across the chemical, pharmaceutical, biotechnology, and metallurgy industries, significantly reducing solvent usage.[6] Specifically, polymeric membranes are gaining attention from researchers for gas separation, as they provide higher purity gas streams (*e.g.*, H_2, O_2, N_2, CO_2, CH_4) for industrial use and help to reduce greenhouse gas emissions.[7–10] To promote green development, green solvents have emerged as promising alternatives for extraction and separation processes.[11] The urgency to address CO_2 emission stems from the imminent threat of global warming. According to studies, the world's temperature has increased by 1.5 °C compared to before industrialization.[12] Consequently, it is anticipated that CO_2 emissions will need to be reduced by 45% from 2010 levels by 2030, with the ultimate target to reach net-zero CO_2 emissions by 2050.

The synthesis of membranes often relies on the use of conventional solvents, which pose significant environmental and health risks due to their toxicity, volatility, and non-biodegradability. The switch from traditional solvents to environmentally friendly solvents for membrane manufacture is due to the hazardous effects of conventional solvents such as *N*-methyl-2-pyrrolidone (NMP), *N*,*N*-dimethylformamide (DMF) and *N*,*N*-dimethylacetamide (DMAc). These solvents produce an extensive amount of effluent annually in industry, which contradicts sustainability goals.[13] These solvents have been classified by the European Chemicals Agency (ECHA) as substances of very high concern (SVHC) due to their reproductive toxicity (hazard statement H360D).[14] To comply with regulations and address environmental, health and safety (EHS) issues, it is imperative to explore greener solvent alternatives. In this review, we focus on green solvents that align with the principles of green chemistry and exhibit a combination of characteristics such as low toxicity, high biodegradability, low volatility, minimal environmental persistence, and derivation from renewable or bio-based sources. Additionally, regulatory factors such as compliance with REACH or GHS safety classifications are considered. These criteria are based on solvent selection frameworks, including CHEM21 and the GlaxoSmithKline (GSK) solvent sustainability guide. Green solvents that meet these parameters provide safer, more sustainable alternatives to conventional solvents like NMP, DMF, and DMAc, making them suitable for use in membrane fabrication.[15–17]

Green solvents are defined based on assessments such as CHEM21 and GSK, which evaluate their potential as substitutes for conventional toxic solvents.[18] Recent studies have highlighted γ-butyrolactone (GBL), dimethyl sulfoxide (DMSO), GVL, Cyrene™, Rhodiasolv® Polarclean, Tamisolve® NxG, DESs, ILs, isopropyl alcohol (IPA), and glycerol derivatives as emerging green solvents, accelerating their exploration for use in separation systems.[18–23] Key properties that green solvents must fulfil include exposure potential, safety, incineration

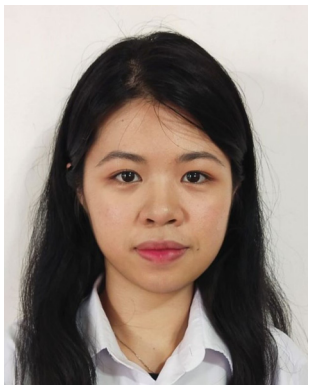

Boon Kee Voon

Boon Kee Voon is currently pursuing a Master's degree in Chemical Engineering at the School of Energy and Chemical Engineering, Xiamen University Malaysia, and is a member of the Centre of Excellence for Green and Advanced Technologies in Efficient Separations (GATES), under the supervision of Prof. Yong. She has served as a research assistant since her final year project in 2020. Her research focuses on environmental impact assessment and the development of sustainable green solvents, particularly for membrane applications in gas separation. She is passionate about integrating environmental considerations into membrane process design to promote greener, more efficient solutions and to advance eco-friendly alternatives that reduce environmental footprints while maintaining high separation performances.

Yen Juin Yap

Yen Juin Yap is an undergraduate student in Chemical Engineering at the School of Energy and Chemical Engineering, Xiamen University Malaysia, and has been supported by the XMUM Merit Scholarship since 2022. She is a research assistant under the supervision of Prof. Yong and a member of the Centre of Excellence for Green and Advanced Technologies in Efficient Separations (GATES). Her academic interests include membrane materials, green separation processes, and sustainable chemical engineering. Currently in the early stages of her research training, she is exploring fundamental concepts in membrane development for environmental applications.

emissions, environmental impact, recovery and recyclability, and low volatility.[24] However, the development of green solvents for incorporation into separation processes is still in its early stages. As shown in Fig. 1, research interest in green solvents for filtration membrane fabrication has grown significantly over the past decade. Despite this progress, further studies are needed to thoroughly assess their environmental impact, underscoring the importance of sustained research efforts in this field.

Particularly for liquid separation, Zou *et al.* provided a thorough review summarizing polymer membranes fabricated with green solvents for water treatment including microfiltration (MF), ultrafiltration (UF), nanofiltration (NF) and reverse osmosis (RO).[25] This review highlighted the shift toward non-toxic solvents in polymer membrane fabrication for applications such as water treatment and gas separation. It evaluated green alternatives, considered their economic impact, and offered insights to enhance sustainability in membrane production. Figoli *et al.* presented a critical review of efforts to replace toxic solvents (*e.g.*, DMF, NMP) with greener alternatives like supercritical CO_2 ($ScCO_2$) and ionic liquids.[20] They highlighted advancements in nonsolvent induced phase separation (NIPS) and temperature induced phase separation (TIPS) techniques, while also acknowledging remaining challenges in achieving complete substitution without compromising performance. Naziri Mehrabani *et al.* summarized the green solvents used in polymeric membrane fabrication including bio-source solvents such as Cyrene™, ILs, DESs, DMSO, TamiSolve® NxG and Polarclean for liquid and gas separation.[26] They critically discussed the dissolution of polymers in the solvents and the role of green solvents in modifying the morphology of the membrane to enhance separation efficiency. Despite these valuable contributions, there remains a gap in the classification of green solvents, and a lack of comparative analysis between solvents used in both liquid and gas separation. Additionally, limited attention has been paid to trade-offs such as environmental impact *versus* membrane performance.

Fig. 2 illustrates the upward trend in the number of publications on green solvents indexed in Web of Science, specifically focusing on their application of selected green solvents in membrane synthesis over the past decade. It highlights the growing importance of exploring green solvents across various applications, particularly for enhancing sustainability. The review presents recent advancements in green solvent research over the last 10 years, with special attention being paid to emerging solvents such as GBL, glycerol triacetate (GTA), triethyl phosphate (TEP), 2-methyltetrahydrofuran (2-MeTHF), Cyrene™, GVL, DMSO, Tamisolve® NxG, Polarclean, Agnique® AMD 3 L, ILs, DESs, palm oil, rice bran oil (RBO), and sunflower oil. Among various membrane applications, NF and gas separation membranes are the most widely studied using green solvents, reflecting strong research interest in sustainable water treatment and carbon capture technologies. This review aims to address these gaps by introducing a comprehensive classification framework for green solvents used in membrane fabrication, encompassing both liquid and gas separation applications. This approach enables a clearer comparison of solvent performance, compatibility with various polymers, and environmental sustainability. With this, the green solvents are categorized as esters, polar aprotic, dipolar aprotic, polar protic, non-polar aprotic, ketones, alcohols, organic salts, and oils. The classification, physicochemical properties, and membrane-related applications of these green solvents in both gas and liquid separation processes are examined. Key advancements in solvent–polymer compatibility, particularly through the use of the Hansen solubility parameter (HSP), are discussed alongside the prevailing challenges in scalability and economic feasibility. Moreover, several AI modelling tools that aid in solvent selection by predicting compatibility and optimizing formulations are discussed. Finally, future prospects are outlined, with the goal of bridging the gap between laboratory research and industrial implementation, thereby accelerating the adoption of sustainable separation technologies.

Wai Fen Yong

Wai Fen Yong is a Professor and Head of Programmes (MSc and PhD in Chemical Engineering) at the School of Energy and Chemical Engineering, Xiamen University Malaysia, and Director of the Centre of Excellence for Green and Advanced Technologies in Efficient Separations (GATES). Her research focuses on sustainable green materials, membranes, and separation technologies. She has received numerous national and international awards, including the National Outstanding Researcher Award (Private Education Cooperative of Malaysia (Educoop)), the 2024 Distinguished Women Scientist Award (ISPT, Elsevier), recognition among the World's Top 2% Scientists by Stanford University in 2023–2024, the 2016 Green Talents Award, and inclusion among the Top 50 outstanding Green Talents alumni from the German Federal Ministry of Education and Research (BMBF).

2. Polymer–solvent interactions

The selection of an appropriate polymer–solvent system is critical for fabricating membranes with tailored porosity, permeability, and selectivity. Hansen solubility parameters (HSPs) serve as a valuable tool for evaluating polymer–solvent affinity by considering the molecular interaction forces involved.[27] This approach enables precise control over phase inversion processes and the resulting membrane morphology, thereby enhancing both performance and reproducibility in membrane fabrication.[28]

HSPs are an extension of the Hildebrand solubility parameter, which quantifies the cohesive energy density of a

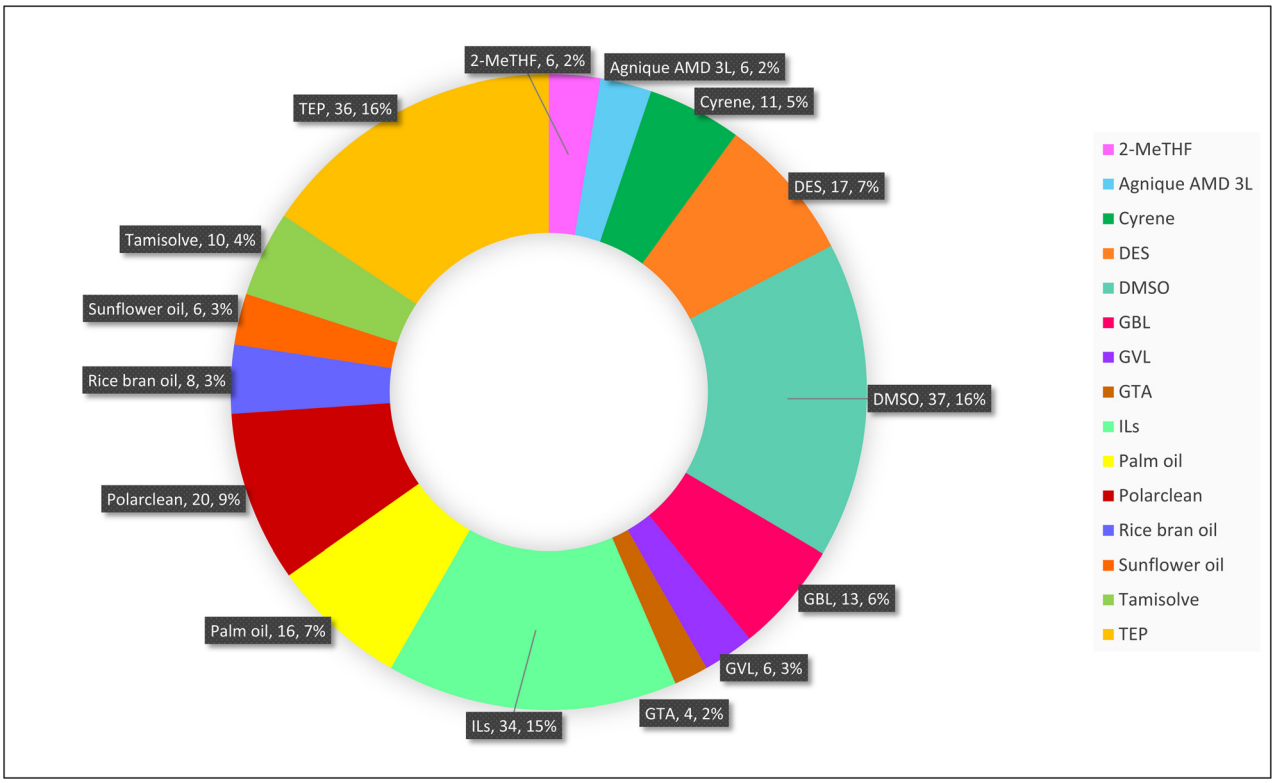

Fig. 1 The number of publications on filtration membranes for each green solvent over the last decade. The green solvents that were searched for on Web of Science using individual terms included 2-MeTHF, Agnique® AMD 3L, Cyrene™, DES, DMSO, GBL, GVL, GTA, ILs, palm oil, Polarclean, RBO, sunflower oil, Tamisolve® NxG, and TEP [accessed on 24 November 2024].

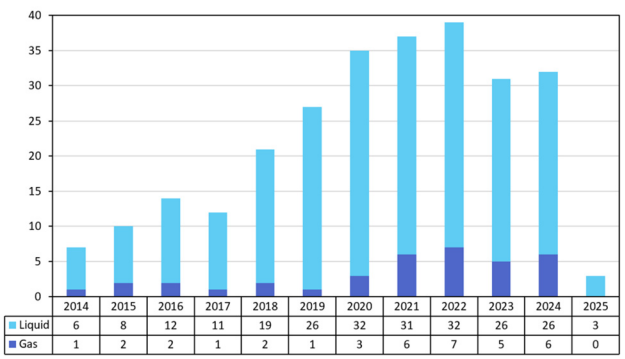

Fig. 2 Publications on filtration membranes using green solvents for each year segregated by gas separation or liquid separation on Web of Science over the last decade. The green solvents that were searched for by individual terms included 2-MeTHF, Agnique® AMD 3L, Cyrene™, DES, DMSO, GBL, GVL, GTA, ILs, palm oil, Polarclean, RBO, sunflower oil, Tamisolve® NxG, and TEP [accessed on 24 November 2024].

material. The total solubility parameter (δ) integrates three individual components, dispersion forces (δ_d), polar interactions (δ_p) and hydrogen bonding (δ_h), into a single measure of cohesive energy density, and is expressed as:

$$\delta = \sqrt{{\delta_d}^2 + {\delta_p}^2 + {\delta_h}^2} \quad (1)$$

where δ_d, δ_p, and δ_h are measured in $MPa^{0.5}$. Dispersion forces (δ_d) arise from van der Waals interactions and depend on the polarizability of molecules, typically representing relatively weak intermolecular forces. Polar interactions (δ_p) reflect dipole–dipole interactions between molecules with permanent dipole moments. Hydrogen bonding (δ_h) accounts for strong intermolecular interactions resulting from hydrogen bonds.[29]

Table 1 summarizes the HSP values for common polymers such as PVDF, PES, polysulfone (PSf), polyetherimide (PEI), and others. The data reveal distinct solubility characteristics. For instance, poly(vinyl alcohol) (PVA) exhibits a high hydrogen bonding component, indicating a preference for highly polar or protic solvents, whereas polyacrylonitrile (PAN) shows strong polar and dispersive interactions, necessitating solvents with balanced polarity. Table 2 lists the HSP values of green solvents, including bio-derived options like Cyrene™, GVL, and Tamisolve® NxG. By comparing the HSPs of polymers and green solvents, one can select alternative green solvents with high polymer–solvent affinity, which can facilitate desirable phase inversion and membrane morphology.

The compatibility between a solvent and a polymer can be evaluated based on their distance in Hansen space, commonly referred to as the HSP distance, R_a, which is expressed as:

$$R_a = \sqrt{4(\delta_{d2} - \delta_{d1})^2 + (\delta_{p2} - \delta_{p1})^2 + (\delta_{h2} - \delta_{h1})^2} \quad (2)$$

Table 1 HSP of selected polymers

Polymers	δ_d ($MPa^{1/2}$)	δ_p ($MPa^{1/2}$)	δ_h ($MPa^{1/2}$)	δ ($MPa^{1/2}$)	Ref.
PVDF	17.10	12.60	10.60	23.74	30
PES	19.60	10.80	9.20	24.20	30
PSf	18.84	11.22	7.95	23.32	25
PEI	19.60	7.60	9.00	22.87	20
PI	20.90	11.30	9.70	25.66	30
CA	16.00	7.50	13.50	22.24	30
PVA	17.00	9.00	18.00	26.34	30
PAN	21.70	14.10	9.10	27.43	30
PESU	17.60	10.40	7.80	21.88	31
PDMS	15.24	4.30	2.92	16.10	32
PEO	17.80	0.56	9.10	20.00	33

Table 2 HSP of selected green solvents

Solvents	δ_d ($MPa^{1/2}$)	δ_p ($MPa^{1/2}$)	δ_h ($MPa^{1/2}$)	δ ($MPa^{1/2}$)	Ref.
2-MeTHF	16.90	5.00	4.30	18.14	34
Agnique® AMD 3 L	18.40	12.90	15.90	27.53	35
Cyrene™	18.80	10.60	6.90	22.66	26
DMSO	18.40	16.40	10.20	26.68	36
GBL	18.00	16.60	7.40	25.58	34
GTA	18.35	13.39	0.43	22.72	37
GVL	15.50	4.70	6.60	17.49	38
Polarclean	15.80	10.70	9.20	21.18	39
Tamisolve® NxG	17.20	8.20	5.90	19.95	39
TEP	16.80	11.50	9.20	22.34	40

where R_a is expressed in $MPa^{0.5}$, and the subscripts 1 and 2 refer to the polymer and solvent, respectively. The factor of 4 in the equation accounts for the greater contribution of dispersion forces to the overall solubility behavior compared to polar and hydrogen bonding interactions.

To further illustrate the relative position of a solvent within the solubility space of a polymer, the relative energy difference (RED) is calculated using the following equation:

$$\mathrm{RED} = \frac{R_a}{R_0} \quad (3)$$

where R_0 denotes the radius of the HSP sphere for the polymer, expressed in $MPa^{0.5}$, and represents the maximum allowable distance within which a solvent is considered compatible with the polymer. Table 3 presents the R_0 values for several commonly used polymers, as reported in experimental studies.

To determine polymer solubility in a given solvent, the RED value is used: if RED < 1, the solvent is likely to dissolve the polymer; if RED > 1, it is unlikely to dissolve the polymer. Table 4 tabulates the calculated R_a and RED values for selected green solvents. The concept of the HSP sphere is central to applying HSPs. Each polymer has a unique solubility sphere in three-dimensional space, defined by its δ_d, δ_p, and δ_h values. The sphere represents the range of solvent parameters compatible with the polymer. Solvents with HSP values that fall within the sphere are likely to dissolve the polymer, while those outside the sphere are not. The size of the HSP sphere is determined by the polymer's solubility behaviour across various solvents, using experimental data to distinguish between solvents that lie inside (soluble) and outside (insoluble) the sphere.

Table 3 HSP sphere radius of polymers from published studies

Polymers	R_0	Ref.
PVDF	5.00	30
PES	6.20	30
PSf	5.42	41
PEI	6.00	42

In this review, HSP analysis is employed as a predictive tool for selecting green solvents with high affinity to specific polymers, thereby guiding the choice of primary solvents. In other cases, it is also used as a framework for designing co-solvent systems when single solvents cannot fully dissolve the polymer. Additionally, it serves as a *post hoc* rationalization method to interpret experimental results in relation to polymer–solvent interactions and their effects on membrane structure and performance.[27,43–45] Fig. 3 illustrates the HSP spheres for PVDF, PES, PSf, and PEI, along with the R_a values of various green solvents, including 2-MeTHF, Agnique® AMD 3 L, Cyrene™, DMSO, GBL, GTA, GVL, Polarclean, Tamisolve® NxG, and TEP.

The HSP analysis reveals that polymers such as PVDF, PES, PSf, and PEI exhibit comparable solubility behaviour, each demonstrating compatibility with a range of green solvents. Among these solvents, Cyrene™, Polarclean, and TEP fall within the HSP spheres, indicating good polymer–solvent affinity with all four polymers. Additionally, DMSO, GBL, and Tamisolve® NxG also show compatibility with three of the polymers, while 2-MeTHF, GVL, and Agnique® AMD 3 L exhibit solubility potential for PEI and PVDF. In contrast, GTA does not fall within the HSP sphere, suggesting limited polymer–solvent affinity for PVDF, PES, PSf, and PEI. However, potential applications in other polymer membrane systems are explored later in this review.

While the HSP offers a useful theoretical framework for evaluating polymer–solvent compatibility, it has inherent limitations.[38,46] The HSP model is based on equilibrium thermodynamics and assumes homogeneous polymer–solvent mixtures; this is not always valid in complex casting solutions. It does not account for kinetic factors such as solvent evaporation rate, phase inversion dynamics, or polymer chain mobility, nor can it predict final membrane morphology. These limitations are particularly relevant in membrane fabrication, where non-equilibrium processes dominate. In systems involving ILs or GVL, deviations from ideal thermodynamic behaviour can further challenge the assumptions underlying the model. Therefore, while HSPs can guide initial solvent selection and help explain observed solubility trends, they should be applied with caution and validated experimentally. In such complex systems, combining HSP with tools like ternary phase diagrams, molecular simulations, and dynamic characteriz-

Table 4 The Hansen solubility distance and RED values of the polymers in green solvents

Polymers / Solvents	PVDF		PES		PSf		PEI	
	R_a	RED	R_a	RED	R_a	RED	R_a	RED
2-MeTHF	9.88	1.98	9.32	1.50	8.19	1.51	7.62	1.27
Agnique® AMD 3 L	5.91	1.18	7.42	1.20	8.17	1.51	9.03	1.50
Cyrene™	5.41	1.08	2.81	0.45	1.22	0.23	4.00	0.67
DMSO	4.62	0.92	6.17	1.00	5.72	1.05	9.20	1.53
GBL	5.43	1.09	6.86	1.11	5.66	1.04	9.69	1.61
GTA	10.50	2.10	9.48	1.53	7.89	1.46	10.64	1.77
GVL	9.42	1.88	10.55	1.70	9.43	1.74	9.02	1.50
Rhodiasolv® Polarclean	3.51	0.70	7.60	1.23	6.23	1.15	8.21	1.37
Tamisolve® NxG	6.44	1.29	6.38	1.03	4.91	0.91	5.75	0.96
TEP	1.88	0.38	5.64	0.91	4.28	0.79	6.83	1.14

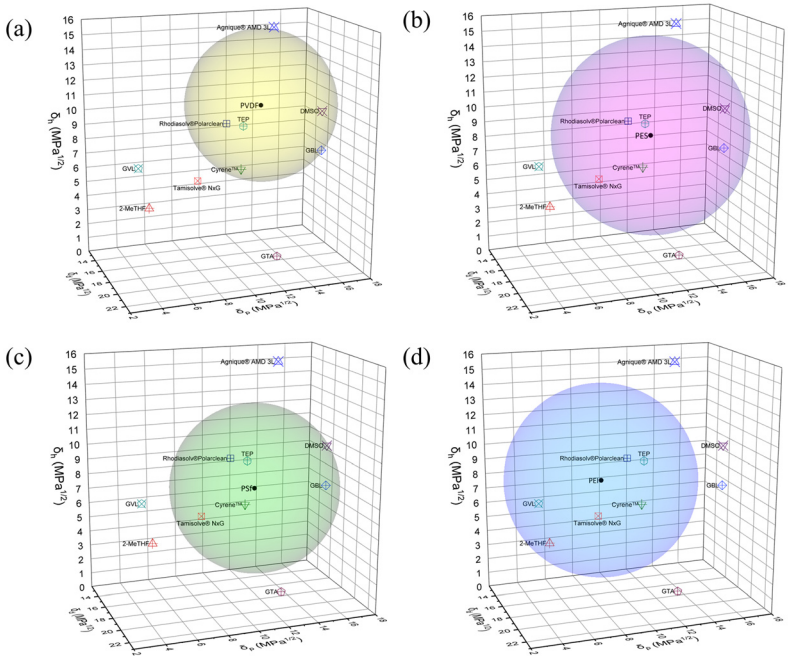

Fig. 3 HSP spheres of a few common polymers, (a) PVDF, (b) PES, (c) PSf, and (d) PEI.

ation techniques provides a more comprehensive understanding of the membrane formation process.

3. Green solvent classification

Green solvents are classified based on their chemical properties and molecular interactions, offering sustainable alternatives to conventional toxic solvents. Generally, they can be categorized as esters, polar aprotic solvents, dipolar aprotic solvents, polar protic solvents, non-polar aprotic solvents, organic salt-based solvents, and oil-based solvents. Table 5 summarizes the properties of these green solvents according to their respective classifications. Esters, such as GBL and GTA, are typically derived from renewable resources and exhibit high biodegradability. Polar aprotic solvents, including TEP, 2-MeTHF and GVL, lack acidic hydrogen but possess significant polarity, making them effective at polymer dissolution. Dipolar aprotic solvents, such as DMSO, Cyrene™, Tamisolve® NxG, and Polarclean, contain two distinct polar centers, enhancing their solvation capabilities. Polar protic solvents, including Agnique® AMD 3 L, contain hydrogen-bond-donating groups, making them suitable for applications involving proton transfer. Organic salt-based solvents, including ILs and DESs, combine low volatility, thermal stability and structural tenability, making them promising for various separation technologies. Lastly, oil-based solvents such as palm oil, rice bran oil, and sunflower oil, utilize naturally occurring lipids and are particularly attractive for use in emulsion liquid membranes. Each solvent class addresses distinct environmental and functional requirements in membrane fabrication, contributing to the advancement of sustainable separation technologies. A summary of solvent availability, production, and costs is presented in Table 6. In this review, the solvent categories

Table 5 Comparison of sustainability attributes of emerging green solvents in membrane separation with their physical properties and environmental characteristics

Class	Green solvents	Molar mass	Density	Melting point	Boiling point	Flash point (closed cup)	Viscosity	NFPA	GHS classification	Toxicity	Waste disposal	Biodegradability	Renewable stocks	Functions in membrane separation	Ref.
Esters	GBL 	86.09 g mol^{-1}	1.13 g cm^{-3} at 20 °C	−43 °C	204 °C	94 °C	Low (1.7 cP)		H302 H318 H336	Moderate	Safe	High	Lignin, cellulose	Applied in flat sheet and hollow fiber membrane preparation	49
	GTA 	218.20 g mol^{-1}	1.161 g cm^{-3} at 20 °C	−78 °C	258 °C	148 °C	Moderate (23 cP)		Not a hazardous substance or mixture	Low	Safe	Moderate	Glycerol	The most CO_2-philic oxygenated hydrocarbon compounds - High CO_2 solubility	50
Polar aprotic	TEP 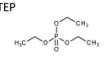	182.16 g mol^{-1}	1.072 g cm^{-3} at 25 °C	−56.4 °C	215 °C	130 °C	Low (1.7 cP)		H319 H302	Slightly moderate	Slightly hazardous	High	Phosphorus trichloride and ethyl alcohol with ammonia gas	Exhibit excellent CO_2 absorption due to dipole–quadrupole interactions Capable of forming hydrogen bonds	51
	2-MeTHF 	86.13 g mol^{-1}	0.855 g cm^{-3} at 20 °C	<−20 °C	78 °C	−10.0 °C	Low (4 cP)		H225 H302 H315 H318	Moderate	Hazardous	High	Sugarcane bagasse, rice straw and corn stover	As a higher boiling substitute for tetrahydrofuran as a solvent for membrane preparation	52
	GVL 	100.1 g mol^{-1}	1.05 g cm^{-3} at 25 °C	−31 °C	206 °C	102 °C	Low (1.86 cP)		H227	Slightly moderate	Safe	High	Cellulose	Applied in CO_2 capture adsorbents	53
Dipolar aprotic	DMSO 	78.13 g mol^{-1}	1.1 g cm^{-3} at 20 °C	16–19 °C	189 °C	87 °C	Low (2 cP)		Not a hazardous substance or mixture	Low	Slightly hazardous	High	Lignin	Promising dipolar aprotic solvent for membranes and adsorbents	54
	Tamisolve® NxG 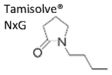	141.21 g mol^{-1}	0.96 g cm^{-3} at 25 °C	<−75 °C	241 °C	108 °C	Low (4 cP)		H302 H315 H319	Moderate	Safe	High	Glutamic acid	Novel solvent for polymeric membrane synthesis	55
	Rhodiasolv® Polarclean 	187.8 g mol^{-1}	1.01 g cm^{-3} at 20 °C	<−60 °C	278–282 °C	144–146 °C	Moderate (9.82 cP)		H319	Slightly moderate	Safe	High	Byproduct of Nylon-66 manufacturing	Solvent for membrane preparation	56 and 57
	Cyrene™ 	128.13 g mol^{-1}	1.25 g cm^{-3} at 20 °C	<−20 °C	227 °C	108 °C	Moderate (14.5 cP)		H319	Slightly moderate	Safe	High	Cellulose	Applied in CO_2 capture adsorbents	58
Polar protic	Agnique® AMD 3 L 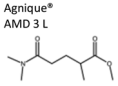	117.1 g mol^{-1}	1.046 g cm^{-3} at 20 °C	≥−11 to ≤2 °C	≥224 °C	109.5 °C	Low (5.1 cP)		Not a hazardous substance or mixture	Low	Safe	High	Lactic acid from fermentation	Solvent for membrane synthesis for a variety of applications, including ultrafiltration and forward osmosis	57 and 59

Table 5 *(Contd.)*

Class	Green solvents	Molar mass	Density	Melting point	Boiling point	Flash point (closed cup)	Viscosity	NFPA	GHS classification	Toxicity	Waste disposal	Biodegradability	Renewable stocks	Functions in membrane separation	Ref.
Organic salt	ILs	—	—	—	—	—	Low	N/A	Non hazardous	Low	Safe	Moderate	Lignin, protein, cellulose, fats	A wide variety of CO_2 philic functional groups such as $-NH_2$, –OH and –COOH	
	DES	—	—	—	—	—	Low	N/A	Non hazardous	Low	Safe	High	Lignin, protein, cellulose, fats	Alternative to toxic amine solvents in industry Capable of forming carbamate	
Oil	Palm oil	847.78 g mol^{-1}	0.88 g cm^{-3} at 20 °C	25–40 °C	>350 °C	>300 °C	Moderate (25 cP)		Not a hazardous substance or mixture	Low	Safe	High	Oil palm	Used as a non-volatile and renewable diluent in emulsion liquid membranes	60
	Rice bran oil	867.90 g mol^{-1}	0.89–0.94 g cm^{-3}	−15 °C	>230 °C	>130 °C	Moderate (47.90 cSt)		Not a hazardous substance or mixture	Low	Safe	High	Rice bran	Used as a solvent in green emulsion liquid membranes	61
	Sunflower seed oil	886.5 g mol^{-1}	0.91–0.93 g cm^{-3}	−15 °C	>230 °C	>93.3 °C	No data available		Not a hazardous substance or mixture	Low	Safe	High	Sunflower seed	Used as a solvent in green emulsion liquid membranes	62

are not always mutually exclusive; classification is based on the most functionally relevant role in membrane processes. Solvents are classified according to their dominant physicochemical behaviour relevant to membrane fabrication, particularly their interaction with polymers and their solvation properties. While some solvents may structurally belong to more than one group, for instance, Cyrene™ is a lactone derivative but also functions as a dipolar aprotic solvent, it has been classified as dipolar aprotic solvent based on its dominant functional behaviour in the context of membrane fabrication. This approach ensures practical relevance to solvent–polymer compatibility and membrane formation dynamics, even though some chemical overlap between groups may exist.

4. Esters

Esters represent a class of green solvents synthesized from renewable biomass, characterized by low toxicity, high biodegradability, and tunable physicochemical properties. Their structural versatility, coupled with CO_2-philic behaviour, makes them particularly suitable for membrane fabrication in both gas and liquid separation processes. This section focuses on two representative ester-based green solvents, namely GBL and GTA, highlighting their synthesis routes, key physicochemical attributes, and potential applications in sustainable membrane processes.

4.1 γ-Butyrolactone (GBL)

γ-Butyrolactone (GBL) is a biomass-derived green solvent produced from glucose *via* catalytic hydrogenation and cyclization processes.[47] It has a relatively high boiling point of 204 °C, making it suitable for high-temperature membrane fabrication and processing applications. Besides, GBL can be synthesized from biomass-derived succinic acid through catalytic hydrogenation followed by cyclization.[48] However, this conventional process typically requires high operational pressures, reaching up to 150 atm, which limit its sustainability and scalability. A greener alternative involves the fermentation of 1,4-butanediol (BDO), offering a more environmentally friendly and potentially cost-effective route to GBL production (Fig. 4). Genomatica, a San Diego-based biotechnology company, reported a new bioprocess for the direct production of BDO from sugar.[48] In this context, the use of a carbon-supported ruthenium (Ru) catalyst to convert BDO into GBL *via* dehydrocyclization is considered more advantageous than the conventional hydrogenation of maleic acid. This BDO-to-GBL conversion process exhibits high efficiency, achieving a GBL selectivity and conversion rate of 99% under optimal conditions of 250 °C and 1 atm. Furthermore, GBL is regarded as a sustainable solvent, as it produces no waste, and the by-products generated during synthesis can be recovered and purified for reuse. Recent studies have demonstrated the potential of GBL as a green alternative to conventional toxic solvents in the fabrication of both flat sheet and hollow fiber membranes for CO_2 capture applications.[85,86]

Table 6 Summary of availability, production and cost of solvents

	Solvent	Availability (no. of vendors)	Production (k tons per year)	Cost (€ per L)	Ref.
Conventional	NMP	71	50–125	130	63–65
	DMF	52	959	130	63, 65 and 66
	DMAc	63	50–60	110	63, 65 and 67
Green	GBL	30	130	85	63, 65 and 68
	GTA	70	10–50	110	63, 65 and 69
	TEP	61	7	125	63, 65 and 70
	2-MeTHF	53	10	81	63, 71 and 72
	Cyrene™	30	1[a]	195	63, 65 and 73
	GVL	71	35[b]	135	63, 74 and 75
	DMSO	60	—	290	63 and 75
	Tamisolve® NxG	63	—	79	63 and 72
	Rhodiasolv® Polarclean	12	—	—	63
	Agnique® AMD 3 L	41	—	60	63 and 72
	ILs	—	0.6[c]	1–30[d]	76 and 77
	DES	—	13.8	—	78
	Palm oil	—	89 287	0.79–1.03	79 and 80
	Rice bran oill	—	11 023	1.16	81 and 82
	Sunflower Seed oil	—	20 966	0.87	83 and 84

[a] It refers to a plant from Circa Group. [b] The GVL production plant is simulated using Aspen Plus. [c] It refers to a plant from Solvionic. [d] The unit is € per kg.

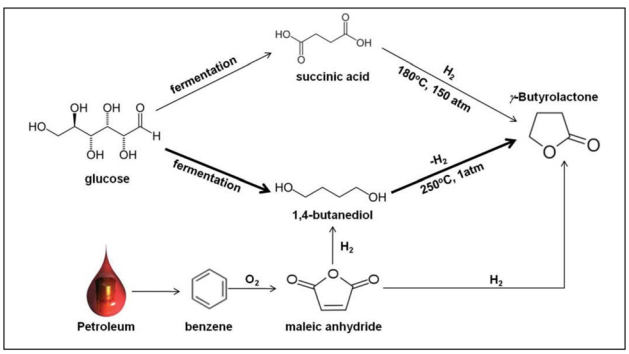

Fig. 4 Production routes for GBL from petroleum- and glucose-based sources. Reproduced from ref. 48 with permission from Royal Society of Chemistry, copyright 2011.

4.2 Glycerol triacetate (GTA)

Glycerol triacetate (GTA), also known as triacetin, is a green solvent made from glycerol through acetylation, a process commonly linked to biodiesel production.[87] It is a colourless, odourless, and viscous liquid with a boiling point of 258 °C. GTA can be synthesized using acetic anhydride and Amberlyst-15 acid resin as a catalyst, achieving nearly 100% yield and its FTIR spectrum matches that of standard GTA (Fig. 5(a)).[88] The U.S. Food and Drug Administration (FDA) has classified GTA as "generally recognized as safe" (GRAS) for use in food, indicating its low toxicity and sustainable nature (Fig. 5(b)).[89,90] It is also considered non-toxic in animal studies involving oral or dermal exposure. GTA is biodegradable, with more than 76% breaking down after 29 days at room temperature. It is widely used in making polyesters, cosmetics, pharmaceuticals, and biodiesel. Due to its oxygen-rich structure, GTA is CO_2-philic, meaning it can dissolve large amounts of CO_2, which are 5 to 6 times higher than diesel oil or water, making it a promising solvent for CO_2 capture.[88,90]

4.3 Applications of ester-based solvents in gas separation

GBL has been employed as a green solvent in the preparation of support membranes for gas separation. Theodorakopoulos *et al.* developed a novel dual-layer graphene nanoplatelet (GNP) mixed matrix hollow fiber membrane by incorporating BTDA-TDI/MDI (P84) as a porous support *via* dry-jet wet phase inversion, followed by dip-coating with Pebax 1657 as the selective layer.[85] GNPs were embedded in both layers, with GBL partially replacing NMP in the dope solution and fully substituting NMP in the bore solution. The incorporation of GNPs increased the ultimate tensile strength of the support layer due to enhanced interfacial adhesion. The resulting membrane showed significantly improved CO_2/CH_4 and He/N_2 selectivity, as well as increased CO_2 and H_2 permeance compared to membranes prepared using conventional solvents with the same selective layer. These improvements were ascribed to the increased fractional free volume (FFV) of the membrane, engendered by disruption of the polymer chains by GNPs. The findings highlight the potential of GBL as a green solvent substitute and GNPs as effective fillers for enhancing gas separation performance. Theodorakopoulos *et al.* further investigated the complete substitution of NMP with GBL in the fabrication of P84 hollow fiber membranes *via* dry-jet wet phase inversion.[91] The resulting membranes demonstrated a CO_2/CH_4 selectivity of 25.7 and CO_2 per-

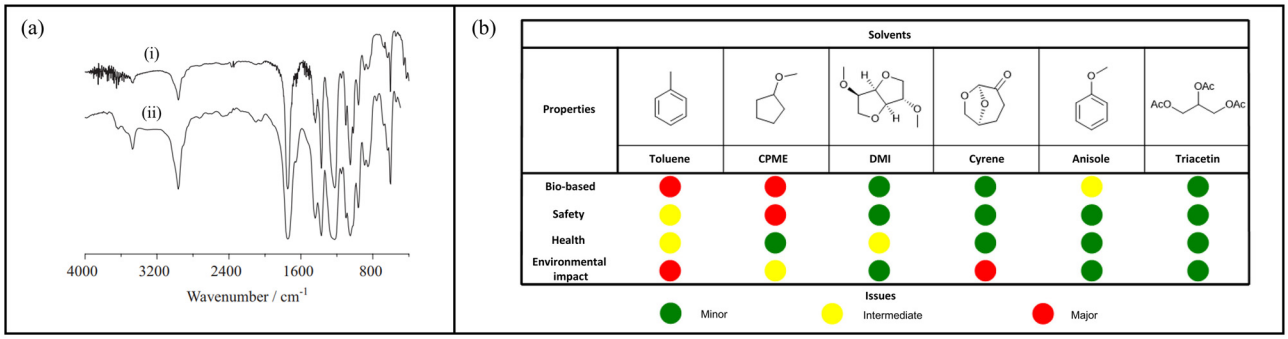

Fig. 5 (a) FITR spectra of (i) standard GTA and (ii) GTA synthesized using a 1 : 3 molar ratio of glycerol to acetic anhydride with Amberlyst-15 acid resin. Reproduced from ref. 87 with permission from PubliSBQ, copyright 2015. (b) Sustainability assessment of GTA compared to toluene, cyclopentyl methyl ether (CPME), dimethyl isosorbide (DMI), Cyrene™ and anisole. Reproduced from ref. 90 with permission from American Chemistry Society, copyright 2025.

meance of 0.38 GPU, showing performance comparable to membranes fabricated using conventional NMP solvents.[91–95] This supports the feasibility of GBL as a greener alternative in hollow fiber membrane production.

Beyond use as a support membrane solvent, GBL has also been utilized for fabricating dense selective layers. Alqaheem and Alomair reported a reduction in the performance of PEI membranes when GBL alone was employed to dissolve the polymer.[96] This decline was attributed to the formation of a dense membrane structure caused by limited interaction between the polymer and GBL, resulting in coiled chains and low chain extension. To address this, they explored the co-use of GBL and DMF (a non-green solvent). Interestingly, membranes prepared with 75 wt% DMF and 25 wt% GBL showed higher permeability than those prepared with 100 wt% DMF. The H_2/CH_4, H_2/N_2, He/CH_4, He/N_2, CO_2/CH_4 and CO_2/N_2 selectivity increased to 29.3, 7.6, 22.6, 5.8, 8.8 and 2.3, respectively. They concluded that further research was needed to identify fully green solvents that could replace DMF.

Zhao *et al.* fabricated Pebax 1657 mixed matrix membranes (MMMs) incorporating carbon nanotubes (CNTs) and GTA for gas separation.[97] CNTs were selected due to their exceptional mechanical strength and ability to enhance gas transport. GTA acted as a plasticizer, enhancing the amorphous structure and chain mobility of Pebax 1657, which in turn improved the CO_2 permeability. However, increasing the GTA content led to a decrease in CO_2/CH_4 selectivity from 17.8 to 14 due to the increase in FFV, which facilitated CH_4 transport. Conversely, an increase in CO_2/H_2 selectivity was observed, which was attributed to improved solubility selectivity.

Another group developed Pebax 1657-based nanocomposite membranes by incorporating alumina nanotubes (ANTs) and GTA.[98] Compared to pristine Pebax, the Pebax/4 wt% ANTs/40 wt% GTA membrane exhibited a 73.8% increase in gas permeability, while the CO_2/CH_4 selectivity decreased only slightly by about 5% to 17.3. This enhancement was ascribed to the porous ANTs disrupting polymer chain packing, thereby increasing FFV and chain mobility.

4.4 Applications of ester-based solvents in liquid separation

For the nanofiltration of rose bengal (RB) dye, 2-MeTHF was employed as a co-solvent in the fabrication of CA membranes, using GTA as the primary solvent.[99] The solubility limit of CA in GTA was found to be approximately 13 wt%. Membranes prepared with GTA and varying concentrations of 2-MeTHF exhibited porous structures characterized by a spongy matrix interspersed with a few large, tear-shaped macrovoids, as illustrated in Fig. 6(a). As the concentration of 2-MeTHF in the casting solution increased, the number of these macrovoids decreased, and the remaining macrovoids adopted a more spherical morphology. To evaluate the effect of 2-MeTHF as a co-solvent, a base casting solution containing 13 wt% CA in GTA was used.

5. Polar aprotic

Polar aprotic solvents are characterized by their high polarity and the absence of acidic hydrogen atoms (*i.e.*, no O–H or N–H bonds). These solvents are widely used in chemical synthesis, polymer dissolution, and membrane fabrication due to their ability to stabilize charged intermediates and dissolve a broad range of polar compounds without engaging in hydrogen bonding. Unlike protic solvents (*e.g.*, water and alcohols), polar aprotic solvents exhibit low nucleophilicity, making them ideal for reactions involving strong bases or nucleophiles. In membrane technology, traditional polar aprotic solvents such as tetrahydrofuran (THF) have been favored for their excellent polymer-dissolving capabilities. However, increasing environmental and health concerns regarding their toxicity, persistence, and reliance on petroleum-based feedstocks have spurred the search for bio-based and greener alternatives. This section explores three promising sustainable polar aprotic solvents, TEP, 2-MeTHF, and GVL with a focus on their production pathways, physicochemical properties, and emerging applications in gas and liquid separation membranes.

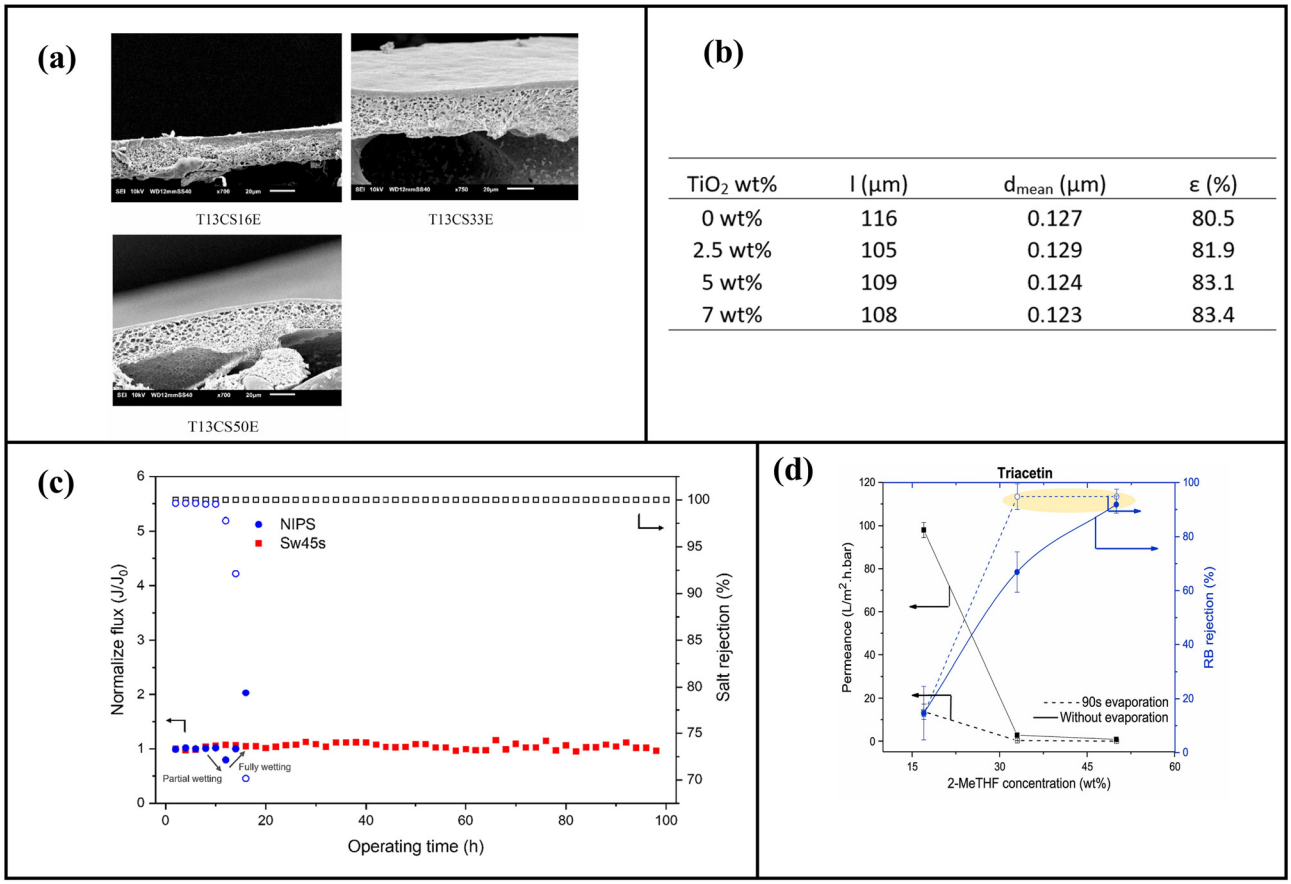

Fig. 6 (a) SEM images of CA membranes prepared using GTA with varying 2-MeTHF concentrations. Reproduced from ref. 99 with permission from Elsevier B.V., copyright 2021. (b) Results of characterization studies on membranes doped with different wt% TiO_2 nanoparticles. Reproduced from ref. 116 with permission from Elsevier B.V., copyright 2024. (c) DCMD performance of NIPS and SANIPS membranes sprayed with water for 45 s (denoted as Sw45s). Reproduced from ref. 102 with permission from Elsevier B.V., copyright 2023. (d) Plot of 2-MeTHF concentration *versus* permeance and dye rejection for CA membranes prepared with GTA. Reproduced from ref. 99 with permission from Elsevier B.V., copyright 2021.

5.1 Triethyl phosphate (TEP)

Triethyl phosphate (TEP) was first investigated as a green alternative to toxic solvents like NMP and DMF for membranes in 2014.[100] TEP is a clear, colourless liquid with the formula $OP(OEt)_3$ and it has a mild, pleasant odour due to its ester structure.[101] It is miscible with water, ethanol, and ether. TEP is recognized for its low toxicity, low volatility (*e.g.*, 1.7 cP), high boiling point (*e.g.*, 215 °C), ease of recovery, and reduced environmental impact.[102] It is widely used in the production of pesticides, polymers, and anhydrides, as a flame retardant,[103] and as a plastic strengthener.[20] In membrane science, TEP has garnered significant interest, particularly for fabricating PVDF membranes. However, due to differences in polarity, solvent strength, and exchange kinetics during phase inversion, TEP exhibits notable differences from NMP, as shown in the ternary phase diagram (Fig. 7(a)), mean squared displacement plot (Fig. 7(b)), and molecular dynamics simulations (Fig. 7(c)).[102,104,105] The ternary phase diagram of PVDF with NMP and TEP indicates that less TEP is required to induce phase inversion of PVDF, as TEP is a weaker solvent compared to NMP.[104] This weaker solvent–solvent–polymer interaction promotes a more coiled polymer chain conformation, leaving a greater free volume between chains, which facilitates the formation of more porous membranes with spongy or honeycomb-like structures. Despite these differences, TEP remains a strong candidate as a sustainable solvent for green membrane fabrication.

5.2 2-Methyltetrahydrofuran (2-MeTHF)

2-Methyltetrahydrofuran (2-MeTHF) is a heterocyclic organic compound that has garnered increasing attention as a bio-derived and potentially greener alternative to conventional solvents in various applications, including membrane fabrication. It can be synthesized from renewable resources such as lignocellulose biomass (Fig. 8), making it a more sustainable option compared to petroleum-based solvents. Moreover, 2-MeTHF exhibits lower toxicity than some commonly used solvents like DCM and NMP.[106,107] Its relatively low boiling point of 78 °C facilitates easier removal and recovery, enhancing its practical appeal in membrane processes. In membrane fabrication,

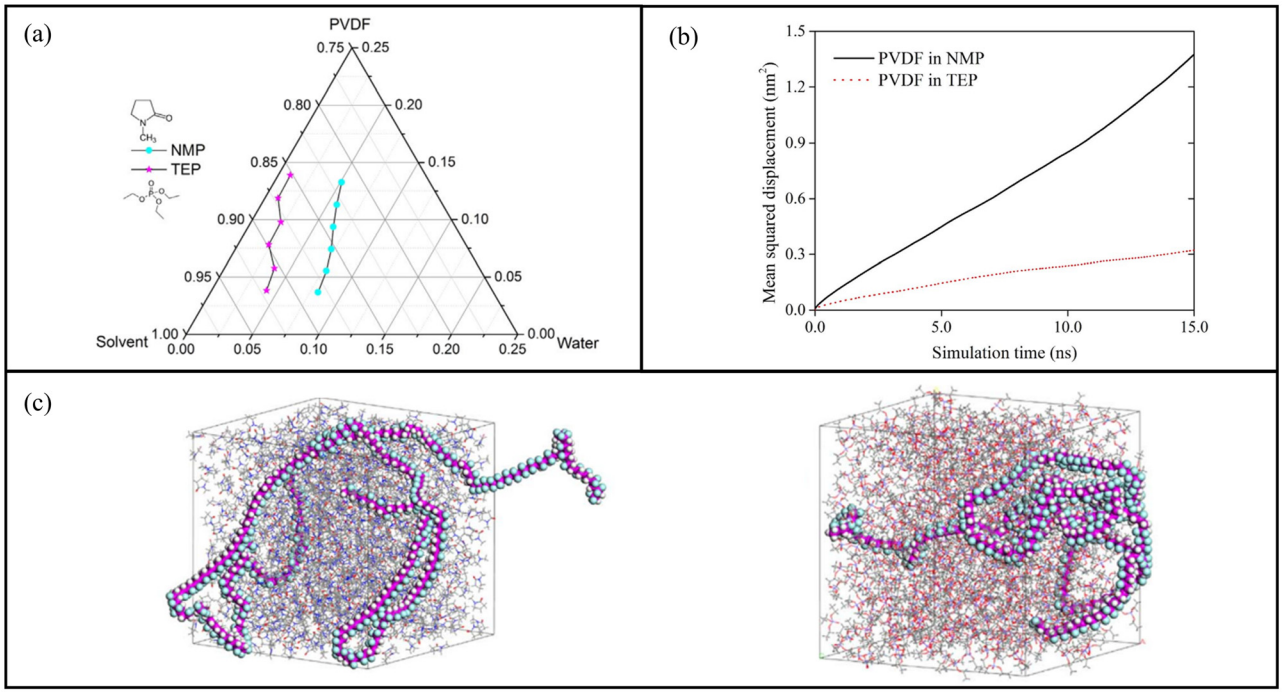

Fig. 7 (a) Phase diagram of the PVDF/solvent/water ternary system. (b) Mean squared displacement (MSD) of PVDF polymer chains in NMP and TEP solvents. (c) Molecular dynamics simulations showing PVDF chain conformations in NMP (left) and TEP (right). Reproduced from ref. 104 with permission from Elsevier B.V., copyright 2017.

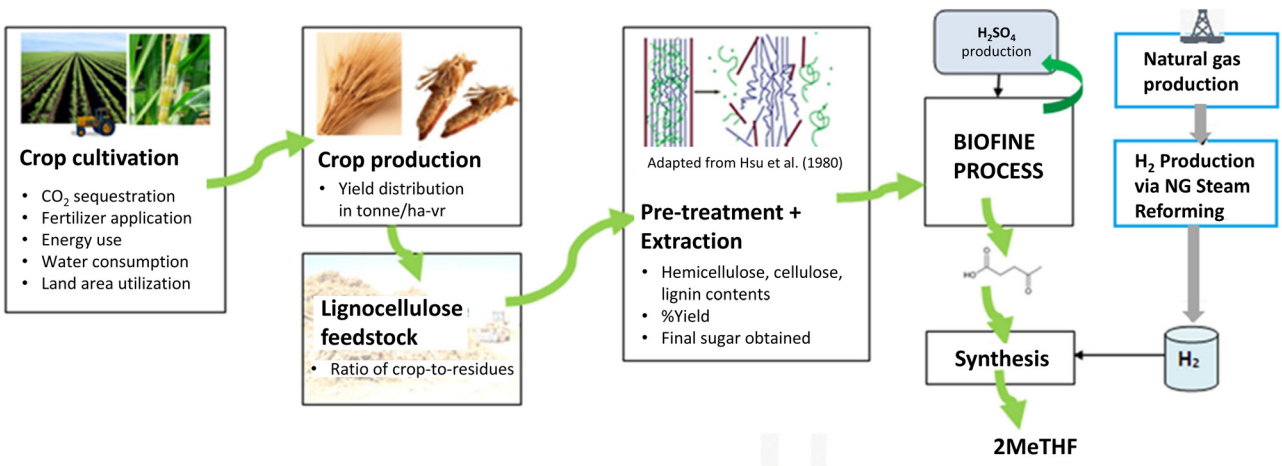

Fig. 8 Life cycle production stages of biomass cultivation to 2-MeTHF production. Reproduced from ref. 107 with permission from Elsevier B.V., copyright 2015.

2-MeTHF can be employed in phase inversion techniques such as NIPS. For instance, it has been used as a co-solvent to dissolve Matrimid®, followed by immersion in a non-solvent bath to initiate phase separation and form the membrane structure. In a study by Shenoy *et al.*, the incorporation of 2-MeTHF as a volatile co-solvent significantly enhanced the CO_2/CH_4 selectivity from 11.5 to 24.0.[108] Despite its promising attributes, the use of 2-MeTHF in membrane fabrication remains relatively underexplored compared to established solvents like NMP. Additionally, considerations such as the cost and commercial availability of 2-MeTHF may influence its feasibility for large-scale membrane production.

5.3 γ-Valerolactone (GVL)

γ-Valerolactone (GVL) is a colorless liquid characterized by low viscosity, a high boiling point (206 °C), and a low melting point (−31 °C), making it stable and liquid under ambient conditions.[109] GVL is also noted for its low flammability and

minimal health hazards. Recognized as an environmentally benign solvent, GVL offers favorable polarity, low toxicology (*e.g.*, oral LD_{50} in rats: 8800 mg kg^{-1}), and most importantly, can be synthesized from biomass sources.[110] GVL is typically produced from levulinic acid, which is derived from hexose sugars. In this process, cellulosic biomass such as corn stover, sawgrass, and wood is hydrolyzed into glucose and other monosaccharides using acid catalysts.[111] These sugars are then dehydrated to form hydroxymethylfurfural, which subsequently yields formic acid and levulinic acid. Levulinic acid can then be converted into GVL *via* two possible reaction pathways (Fig. 9(a)).[110] Experimental assessments of the biodegradability of GVL suggest it can be rapidly and completely degraded in the environment.[112] Moreover, its low volatility and flammability under standard conditions have made it a widely used functional solvent in various applications. Most reported studies have focused on its application in the synthesis of CO_2 sorbents, indicating the need for further exploration of its potential in direct gas separation and capture technologies.[110,113–115]

5.4 Applications of polar aprotic-based solvents in gas separation

In a recent study by Shenoy *et al.*, a green solvent system comprising Tamisolve® NxG, DMSO and 2-MeTHF was employed to fabricate polyimide Matrimid® membranes for biogas purification, specifically targeting CO_2/CH_4 separation.[108] Among the components, DMSO introduced thermodynamic instability due to its limited affinity for Matrimid® and strong affinity for water. In contrast, Tamisolve® NxG and 2-MeTHF demonstrated better compatibility with the polymer matrix. Membranes were fabricated using this ternary solvent system, with increasing concentrations of 2-MeTHF as a volatile co-solvent, while maintaining a fixed 1 : 2 ratio of Tamisolve® NxG : DMSO. The gas separation performance was evaluated using a 50 : 50 vol% CO_2/CH_4 mixed gas feed. The membrane fabricated with 24 wt% 2-MeTHF demonstrated a notable improvement in CO_2/CH_4 selectivity from 14.0 to 22.0. However, this enhancement was accompanied by a reduction in CO_2 permeance, which decreased from 170 to 144 GPU. This study highlights the potential of green solvent systems in optimizing membrane performance for sustainable gas separation applications.

5.5 Applications of polar aprotic-based solvents in liquid separation

In recent years, TEP has been explored as a green solvent for membrane distillation (MD). Santoro *et al.* utilized TEP in the fabrication of PVDF membranes doped with TiO_2 nanoparticles for MD, integrated with the photooxidation of arsenite (As(III)) to arsenate (As(V)) for freshwater recovery.[116] The fabricated membranes exhibited high porosity (ε), exceeding 80%, and a narrow pore size distribution, with a mean pore size (d_{mean}) of 0.123–0.129 μm, as shown in Fig. 6(b), when different loadings of TiO_2 were added to the PVDF membrane fabrication process for water treatment. The thickness of the membranes (l) falls in the range of 105–116 μm.

These PVDF membranes featured an asymmetric structure with a finger-like top layer and a spherulitic substructure, resulting in different hydrophobicity, in which the contact angles measured around 120° on the rougher spherulitic side and around 92° on the smoother finger-like side. Vacuum membrane distillation (VMD) experiments demonstrated the membrane's ability to recover over 80% of water from arsenic-contaminated solutions while achieving a fivefold concentration of As(III). Transmembrane flux increased from 1.2 ± 0.1 kg m^{-2} h^{-1} to 6.3 ± 0.3 kg m^{-2} h^{-1} as the feed temperature increased from 40 °C to 60 °C, further improving to 7.1 ± 0.2 kg m^{-2} h^{-1} under UV irradiation due to additional radiant heating.

Moreover, Chung and co-workers successfully developed superhydrophobic PVDF membranes using TEP as a green solvent *via* the spray-assisted non-solvent induced phase separation (SANIPS) method for brine desalination through direct contact membrane distillation (DCMD).[102] As the air spray duration increased from 0 to 240 s, the PVDF membranes originally exhibiting a flattened surface morphology showed a gradual decrease in water contact angle from 124° to 82°. This

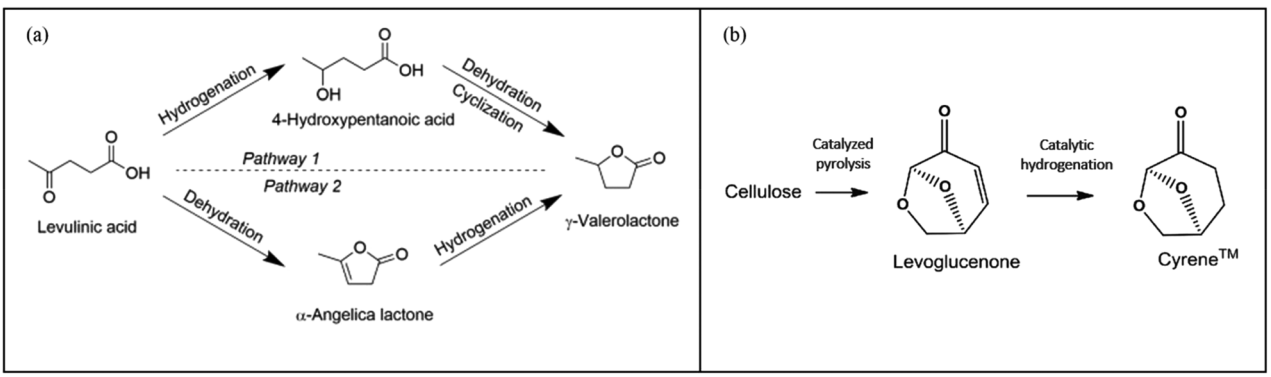

Fig. 9 (a) Two sustainable pathways for the production of GVL. Reproduced from ref. 110 with permission from Elsevier B.V., copyright 2019. (b) Two-step synthesis of Cyrene™. Reproduced from ref. 145 with permission from IntechOpen, copyright 2019.

change was attributed to a slower phase inversion process and Marangoni effects inherent to TEP.[117,118] Notably, membranes sprayed with water for 45 s achieved superhydrophobic surfaces with self-cleaning properties, demonstrating advanced functional performance. The separation performance of membranes fabricated *via* NIPS and SANIPS methods was evaluated using a 10 wt% NaCl solution at 60 °C in a DCMD setup. While the NIPS membrane experienced wetting after 10 h with salt rejection dropping dramatically to 70% within 3 h, the SANIPS membrane treated with water for 45 s maintained a stable water flux of 22 kg m^{-2} h and a high salt rejection rate of 99.9% throughout the 100 h continuous test (Fig. 6(c)).[102] This exceptional performance was attributed to the superior wetting resistance and superhydrophobic characteristics of the membrane.

As previously mentioned, 2-MeTHF was employed as a co-solvent in the fabrication of CA membranes for the nanofiltration of RB dye, with GTA as the primary solvent. The results showed that increasing the 2-MeTHF concentration led to a decrease in permeance but an improvement in RB rejection, as depicted in Fig. 6(d).[99] This trend is attributed to the volatile nature of 2-MeTHF, despite the minimized evaporation time before coagulation.[119] These findings suggest that the addition of 2-MeTHF enhanced membrane selectivity, positioning it as a promising co-solvent for optimizing the nanofiltration performance in dye separation applications. Besides, 2-MeTHF was applied in the cross-linking of polybenzimidazole (PBI) membranes for organic solvent nanofiltration (OSN). The resulting cross-linked PBI membrane demonstrated exceptional performance, achieving a 99.6% rejection rate for Remazol Brilliant Blue R. Additionally, it exhibited high solvent permeances of 40.7, 29.0, 13.8, and 5.8 LMH per bar for acetonitrile, acetone, ethanol, and isopropanol, respectively, under a test pressure of 10 bar. This combination of high rejection and significant solvent permeance highlights the effectiveness of membranes in both separation and solvent filtration applications.[120]

Additionally, Rasool *et al.* reported that GVL was a promising alternative to conventional organic solvents for dissolving polymers such as CA, polyimide, PES, cellulose triacetate (CTA), and PSf.[21] However, they found that chitosan and PVA were insoluble in GVL. NF membranes fabricated using 10% CTA/GVL and 15% CA/GVL achieved 90% rejection of RB with a PWP of 11.7 LMH per bar and 1.8 LMH per bar, respectively. In another study, the same group further confirmed the feasibility of employing GVL as an organic solvent in the NIPS process.[121] The 10% CTA/GVL membrane, using water as the non-solvent, exhibited optimal performance with 94% rejection of RB with a PWP of 15.9 L m^{-2} h^{-1} bar^{-1}.

6. Dipolar aprotic

Dipolar aprotic solvents play a crucial role in membrane fabrication due to their high polarity, strong solvation power, and chemical stability. Unlike protic solvents, they lack acidic hydrogen, making them ideal for dissolving polymers and facilitating phase inversion processes. However, conventional dipolar aprotic solvents such as NMP and DMF pose environmental and health risks due to their toxicity and fossil-fuel origins. This section explores four sustainable alternatives, namely DMSO, Tamisolve® NxG, Polarclean and Cyrene™ that offer comparable performance with reduced ecological footprints. Their successful applications in gas and liquid separation membranes demonstrate their potential to replace traditional solvents while maintaining or even enhancing membrane performance.

6.1 Dimethyl sulfoxide (DMSO)

DMSO derived from lignin, is a biodegradable and non-hazardous solvent.[122] In addition to being extracted from lignin (Fig. 10(a)),[123] it can also be produced *via* the oxidation of dimethyl sulfide (DMS), as shown in Fig. 10(b).[124] DMSO has a boiling point of 189 °C. Notably, the conversion of DMS into DMSO is considered a relatively sustainable process, as it does not require a catalyst, initiator, or photosensitizer, relying instead on an autoxidation reaction.[125] The synthesis pathway is straightforward whereby DMS can be oxidized to DMSO *via* catalytic oxidation at 7.2 MPa and 105 °C.

Key characteristics such as high biodegradability, low toxicity and non-mutagenicity make DMSO a suitable alternative to toxic solvents. Reports indicate that DMSO exhibits exceptionally low human health toxicity, with an estimated burden of less than 0.5×10^{-6} disability-adjusted life years (DALYs) per kilogram of solvent emitted, reflecting its minimal impact on the human population.[126] Moreover, it poses minimal risk to aquatic organisms. For instance, LD_{50} values for salmon and trout range from 12 to 17 g kg^{-1}, while EC_{50} values for aquatic invertebrates and plants are approximately 2–3%. A study by the U.S. Fish and Wildlife Service also classified DMSO as having low toxicity to fish.[127] The U.S. Environmental Protection Agency (EPA) has stated that DMSO is non-toxic and poses no health risks to humans.[128]

Furthermore, DMSO is a low viscosity, polar aprotic and recyclable solvent, making it suitable for diverse applications. For example, DMSO can be used to extract polyester from waste jeans in the textile industry, and the used solvent can be recycled, resulting in a 99% reduction in solvent waste.[129] It is also considered a promising green solvent substitute for toxic solvents in perovskite solar cell production.[126] Due to its high dissolving power for a wide range of polymers, DMSO is more frequently used than other green solvents. Figoli *et al.* reported that none of the green solvents tested, including Polarclean, Tamisolve® NxG, GVL and Cyrene™ were capable of dissolving certain polymers.[20] However, DMSO is the only green solvent demonstrating similar solubility characteristics and polymer–solvent interactions to those of conventional solvents.[130] To date, DMSO has also been utilized in CO_2 capture applications. Its high dissolving power enables the dispersion of various adsorbents for CO_2 capture such as chitin-acetate, α-cyclodextrin and choline glycinate.[131–133] Additionally, dissolving amines in DMSO promotes the formation of carbamate

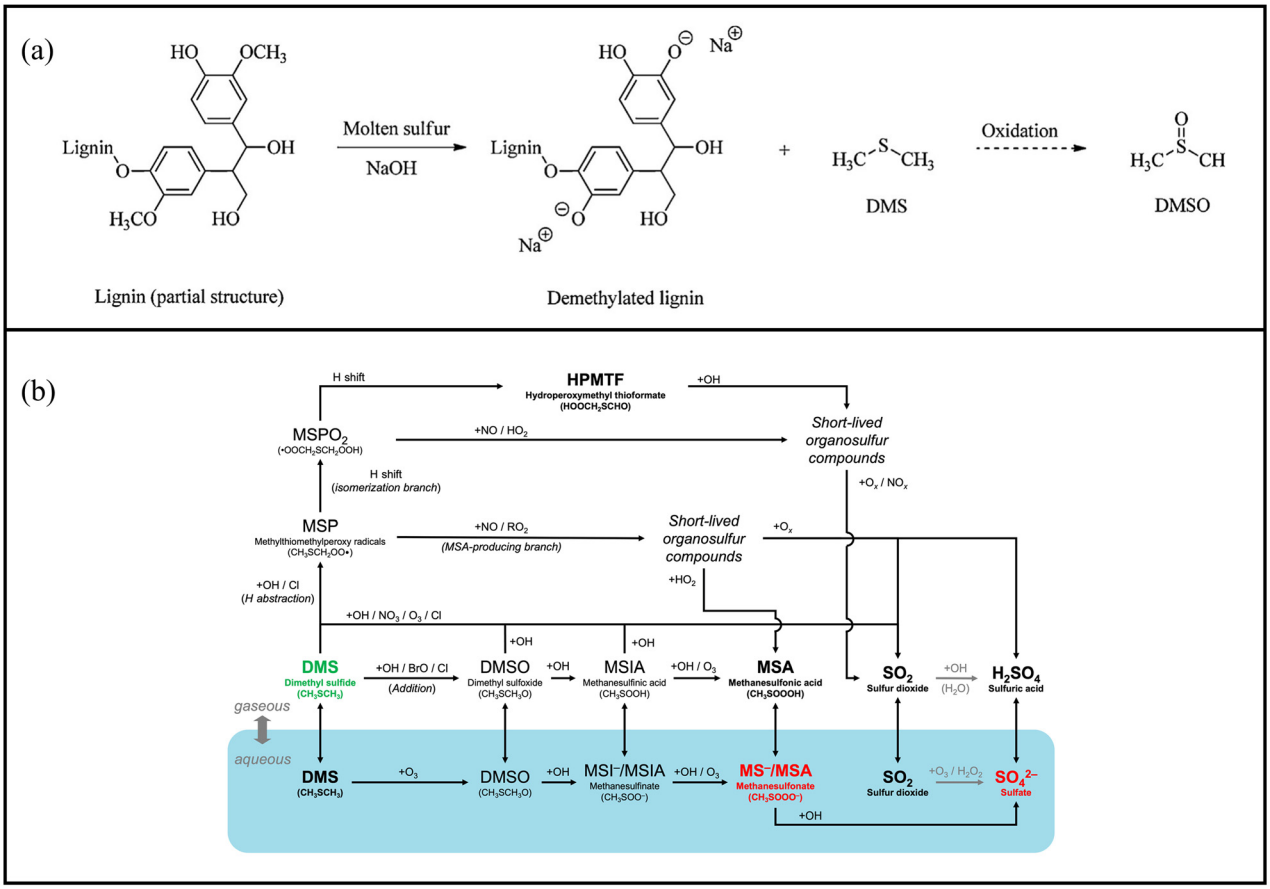

Fig. 10 (a) Chemical modifications occurring during DMSO production from lignin. Reproduced from ref. 123 with permission from Elsevier B.V., copyright 2014. (b) Schematic summary of expanded atmospheric chemistry of DMS oxidation. Reproduced from ref. 124 with permission from Copernicus, copyright 2022.

species upon reaction with CO_2, thereby increasing CO_2 take up.

6.2 Tamisolve® NxG

Tamisolve® NxG is primarily composed of *N*-butyl-2-pyrrolidinone (NBP), which belongs to the same chemical family as NMP, namely *N*-alkyl-2-pyrrolidones, but has a more favourable toxicological profile. According to REACH and the European CLP Regulation (GHS), NBP is not classified as reprotoxic or mutagenic and is not listed as an SVHC.[134] Supplier and regulatory data further indicate that it is inherently biodegradable and has low acute toxicity, making it a promising and safer alternative to NMP in membrane fabrication.[55] As a non-toxic, dipolar aprotic solvent, NBP makes commercially available Tamisolve® NxG a promising green solvent due to its non-mutagenic, inherently biodegradable, and non-reproductively toxic properties.[38] Tamisolve® NxG possesses physical properties similar to other dipolar aprotic solvent, with a melting point below −75 °C, a boiling point of 241 °C, a flash point of 108 °C, and a viscosity of 4 cP.[135] Despite having a longer carbon chain and lower polarity than toxic dipolar aprotic solvents (*e.g.*, NMP, DMF, DMAc, and DMSO), Tamisolve® NxG remains a preferred alternative substitute due to its bio-based, non-toxicity, and biodegradability, all of which contribute to a reduced environmental footprint and improved safety. Tamisolve® NxG has been applied in a range of synthesis processes, including membrane preparation for nanofiltration, synthesis of thin film composite membranes, and solid-phase peptide synthesis.[136] It can also substitute NMP and *N*-ethyl pyrrolidinone in Heck cross-coupling reactions, heterocycle synthesis and benzylation of sodium acetate.[135]

6.3 Rhodiasolv® Polarclean

Rhodiasolv® Polarclean with the IUPAC name methyl-5-(dimethylamino)-2-methyl-5-oxopentanoate is commonly referred to as Polarclean. It is a green solvent with a boiling point between 278 and 282 °C, a melting point of −60 °C, and a flash point between 144 and 146 °C.[137] Polarclean is produced *via* the valorization of 2-methylglutaronitrile (MGN), a byproduct of Nylon-66 manufacturing.[138] It has found application in various fields, including agrochemical formulation, plant protection, animal nutrition, and polymer dissolution (*e.g.*, PSf, PES, CA, PVDF, polyvinyl chloride (PVC), Pebax and

Matrimid®) for membrane fabrication due to its high solvency.[137,139,140] Polarclean stands out as an environmentally friendly alternative to conventional toxic solvents, boasting advantages such as 97% biodegradability within 18 days, low vapour pressure, sustainability, low toxicity and non-mutagenic characteristics.[31,141,142] Ortiz-Albo *et al.* explored the use of Polarclean and found that it had a Hansen solubility parameter closer to those of polymers than to hazardous solvents such as DMF, DMAc, and NMP.[139] They successfully employed Polarclean in membrane preparation for CO_2 capture applications.

For solvent recovery, vacuum distillation proved to be an effective method, enabling high-purity recovery of Polarclean from the aqueous phase at a water : Polarclean volume ratio of 10 : 3.[143] As a less energy-intensive alternative, liquid–liquid extraction was also explored. In this approach, the aqueous mother liquor was first washed with toluene to remove apolar contaminants such as unreacted substrates or products. Owing to its polar nature, Polarclean remained in the aqueous layer, but its moderate polarity also enabled efficient extraction using ethyl acetate (EtOAc). Subsequent evaporation of EtOAc yielded Polarclean with >99% purity, demonstrating its strong potential for reuse *via* both distillation and solvent extraction routes.

6.4 Dihydrolevoglucosenone (Cyrene™)

Dihydrolevoglucosenone (Cyrene™) is a dipolar aprotic solvent synthesized from cellulose in a two-step process.[144] First, cellulose undergoes acid-catalyzed pyrolysis to levoglucosenone (LGO), which is then hydrogenated to produce Cyrene™ (Fig. 9(b)).[145] It can be derived from a variety of biomass such as corn cobs, crude softwood waste, larch logs, bagasse and poplar wood.[146] Recently, Cyrene™ was used by researchers in adsorbent and membrane synthesis.[22,147–150] Notably, Cyrene™ exhibits physicochemical properties comparable to those of toxic, petrochemical-derived solvents such as NMP, particularly in terms of polarity and solubilizing power, making it a promising bio-based substitute.[151] Its versatility is further demonstrated by its applicability in various chemical reactions, including carbon–carbon bond formation, nucleophilic substitution, and the synthesis of ureas and amides. Cyrene™ is also recognized for its favorable environmental profile. It is classified as a safer, environmentally benign solvent, as it does not contain nitrogen or sulfur atoms. Hence, it does not release hazardous by-products like NO_x or SO_x during degradation. Despite these advantages, the application of Cyrene™ in CO_2 capture remains relatively unexplored, and further research is warranted to assess its full potential in this area.[147,148]

Despite its strong green credentials and comparable solubility parameters to DMF and NMP, Cyrene™ presents several practical challenges that limit its widespread adoption. One key drawback is its relatively high viscosity (~14.5 cP at 20 °C), which can affect polymer dissolution and dope solution processability during membrane casting.[152] During the membrane preparation process with Cyrene™, high humidity would cause polymer precipitation and agglomeration.[22] Economic and logistical factors also present barriers. Cyrene™ is currently produced at a limited scale and commercial Cyrene™ contains numerous impurities that can interfere in the process.[153] These trade-offs underscore the need for further process optimization and supply chain development to enable broader use of Cyrene™ in membrane fabrication.

6.5 Applications of dipolar aprotic-based solvents in gas separation

Liu and coworkers developed PSf/SNW-3 MMMs by incorporating a novel Schiff base network (SNW-3) into a PSf matrix.[154] DMSO was used to dissolve melamine and isophthalaldehyde during the synthesis of SNW-3 fillers, as illustrated in Fig. 11(a). The fillers were then mixed with PSf beads in chloroform and subjected to ultrasonic treatment to achieve uniform dispersion. FESEM images of the SNW-3 fillers and resulting MMMs are given in Fig. 11(b). Compared to pristine PSf membranes, PSf/SNW-3 MMMs demonstrated enhanced CO_2/N_2 and CO_2/CH_4 selectivities and permeabilities, surpassing the Robeson upper bound. This improvement is likely to be due to polymer chain rigidification induced by SNW-3, which also enhances membrane resistance to CO_2 plasticization.

Soh *et al.* reported Tamisolve® NxG as a green solvent for fabricating polyimide membranes for CO_2 separation by assessing the solubility of 6FDA-durene using HSPs.[23] They compared two fabrication methods, namely chemical imidization and one-step high-temperature polymerization. Membranes fabricated from polymer synthesized *via* chemical imidization exhibited lower chain packing, higher free volume, and greater gas permeability. In constrast, membranes prepared through one-step polymerization displayed higher thermal stability and molecular weight. The chemically imidized membranes delivered superior gas permeability and O_2/N_2, CO_2/N_2, and CO_2/CH_4 selectivities as shown in Fig. 12,[23] with a CO_2 plasticization pressure reaching up to 25 bar, outperforming those fabricated with conventional solvents.[154–156]

For gas separation, Ortiz-Albo *et al.* employed a hybrid phase inversion method using Polarclean to fabricate self-standing Pebax®1074 membranes at polymer concentrations of 11, 16, and 20 wt%.[139] The resulting membranes exhibited gas separation performance comparable to those prepared with NMP. Increased polymer concentration led to higher crystallinity, reducing CO_2 permeability due to the formation of a more rigid matrix. Notably, the membrane fabricated with 16 wt% polymer achieved a CO_2 permeability of ~150 barrer and a CO_2/N_2 selectivity of ~45, approaching the 2008 Robeson upper bound. This demonstrated the feasibility of replacing NMP with Polarclean in Pebax®1074-based gas separation membranes.

Bridge *et al.* prepared defect-free asymmetric PSf membranes for gas separation using Cyrene™ and tetrahydrofuran (THF) as solvents *via* the NIPS technique.[148] They reported that Cyrene™ effectively suppressed macrovoid formation and produced a rigid, interconnected porous sublayer, unlike mem-

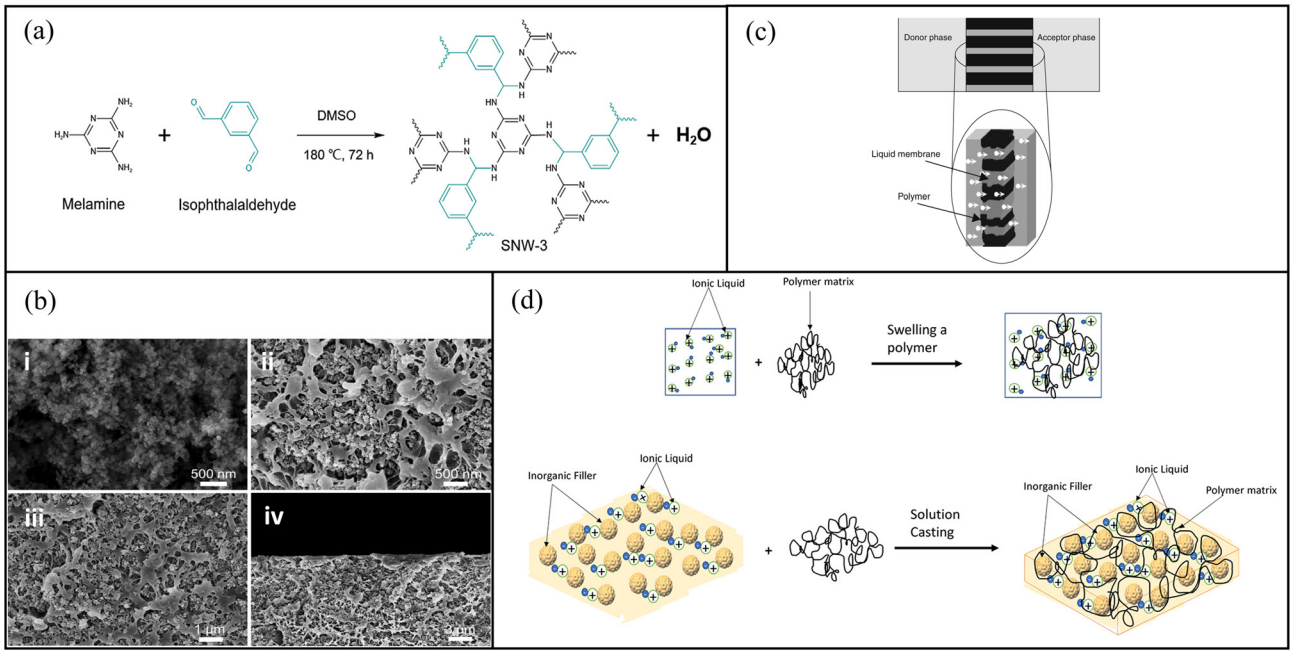

Fig. 11 (a) Schematic diagram of the chemical reaction used to synthesize SNW-3 fillers with melamine and isophthalaldehyde. (b) FESEM images of (i) SNW-3 fillers and (ii–iv) SNW-3/PSf MMMs. Reproduced from ref. 154 with permission from Elsevier, B.V., copyright 2022. (c) Illustration of phases present in supported liquid membranes (SLMs). Reproduced from ref. 155 with permission from Elsevier, B.V., copyright 2010. (d) Synthesis of ILMMMs. Reproduced from ref. 156 with permission from Wiley, copyright 2019.

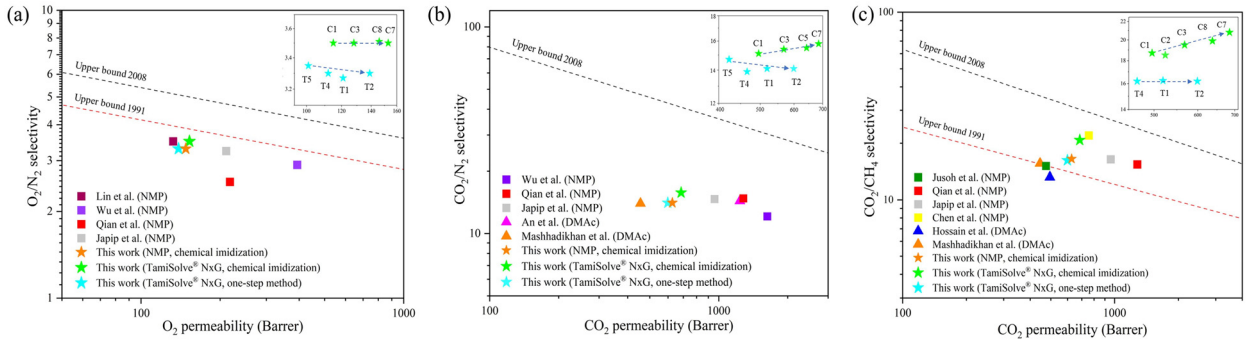

Fig. 12 Comparison of gas separation performance of membranes fabricated using Tamisolve® NxG *versus* conventional solvents, benchmarked against the Robeson upper bound of (a) O_2/N_2 selectivity to O_2 permeability, (b) CO_2/N_2 selectivity to CO_2 permeability, and (c) CO_2/CH_4 selectivity to CO_2 permeability. Reproduced from ref. 23 with permission Elsevier B.V., copyright 2023.

branes prepared using DMAc. Although the gas selectivity of the resulting membranes was slightly reduced, it remained within acceptable limits. Among the membranes developed, the PSf/Cyrene™/THF/EtOH (0.2/0.45/0.19/0.16) membrane with a drying step of less than 10 s achieved the highest H_2/CO_2 selectivity of 2.5 and H_2 permeance of 115 barrer.

Using Matrimid® as the polymer, Bridge *et al.* further explored the development of defect-free asymmetric membranes for gas separation.[147] A similar suppression of macrovoid formation was observed when using Cyrene™ as the solvent. The membrane prepared with 14 wt% Matrimid® and a 5 s drying time exhibited the highest H_2/CO_2 selectivity of 4.1 and an H_2 permeance of 149 GPU at 10 bar. This result outperformed their previous results using PSf and DMAcfor H_2/CO_2 separation.

6.6 Applications of dipolar aprotic-based solvents in liquid separation

Yang *et al.* employed DMSO as a green solvent to dissolve CA for nanofiltration membrane fabrication,[157] DMSO was utilized. The resulting membrane support was subsequently deacetylated using a 0.1 M NaOH solution in ethanol. Ethanol is a bio-based, non-toxic, and biodegradable solvent. This treatment yielded a cellulose with excellent solvent resistance and hydrophilicity, ideal for fabricating thin film composite (TFC) membranes. The solute rejection performance of algal-based

membranes was evaluated using styrene oligomers with molecular weights ranging from 236 to 1900 g mol^{-1}. The TFC membranes exhibited a molecular weight cut-off (MWCO) range of 434 to 880 g mol^{-1} and demonstrated high permeance for polar solvents such as acetone (*e.g.*, from 7.8 to 22.9 L m^{-1} h^{-1} bar^{-1}), while lower permeance was observed for nonpolar solvents, indicating favourable selectivity for polar solvents.[158] The tightest membrane, TFC9, achieved 81.7% rejection of styrene dimer (*e.g.*, 236 g mol^{-1}) and ≥90% rejection of solutes around 505 g mol^{-1}.

DMSO is recognized as a viable solvent for various polymers, including PVDF, PES, polyimide, PAN, PBI, poly(amide-imide) (PAI), CA and poly(vinylpyrrolidone) (PVP).[25] Marino *et al.* validated the use of DMSO EVOL™ as an alternative to NMP for PES membrane fabrication *via* phase inversion.[159] Pore forming polymers such as PVP, Pluronic®, polyethylene glycol (PEG) were utilized, resulting in membranes with enhanced pore size and thickness. Specifically, membranes incorporating PVP/PEG exhibited PWPs ranging from 2000 to 7700 LMH per bar, while those with Pluronic®/PEG reached 3500 to 13 200 LMH per bar. PVP-incorporating membranes also demonstrated superior mechanical properties and thickness compared to Pluronic®-based ones, reinforcing the suitability of DMSO as a substitute for NMP. Similarly, Foong *et al.* demonstrated that DMSO could replace NMP when fabricating PSf membranes using gum Arabic (GA) as an additive.[160] The DMSO-based PSf membranes exhibited comparable PWP to those made with NMP, while maintaining excellent dye rejection (*e.g.*, 84.84%), PWP (*e.g.*, 8.63 LMH) and flux recovery ratio (FRR) (*e.g.*, 93.29%); this was attributed to increased porosity and pore size.

Ong *et al.* further applied DMSO in the preparation of PSf MMMs using graphene oxide (GO) as nanofillers.[161] The inclusion of GO up to 1 wt% loading enhanced membrane porosity, though aggregation at 2 wt% reduced the performance. The optimal membrane with 0.5 wt% GO achieved a PWP of 76.1 LMH, humic acid rejection of 53.5%, and an FFR of 96.2%.

For solvent-resistant membrane applications in dye and pharmaceutical separations, Alqadhi *et al.* dissolved poly (ether-ether-ketone) (PEEK) in Tamisolve® NxG.[162] Cross-linking improved membrane stability up to 15 days at 30 bar. The membranes demonstrated MWCO values of 540 to 768 g mol^{-1} and effectively separated roxithromycin with 99.8% rejection from impurities with minimal API loss during diafiltration. In other work, Jiang *et al.* employed Tamisolve® NxG to develop TFC membranes using PES as the substrate polymer and PEG as a pore-forming agent.[38] Pure water permeability (PWP) measurements for both TFC membranes were performed using a lab-scale dead-end filtration cell at room temperature under an applied pressure of 10 bar and the study was carried out together with membranes prepared with NMP, DMF and DMAc. HSP confirmed the affinity between PES and Tamisolve® NxG. The PES/Tamisolve® NxG/PEG (12/58/30) membrane exhibited the best PWP of 3.54 LMH per bar and NaCl rejection of 92.6%, due to increased porosity and surface roughness resulting from the lower PES concentration and higher PEG content.

To increase hygroscopicity for water vapour absorption, Marino *et al.* developed UF and MFPES membranes using Polarclean combined with PVP and PEG *via* NIPS and VIPS techniques.[31] Sponge-like membranes with bi-continuous morphologies were obtained by adjusting the polymer and additive contents, and air exposure time. Wang *et al.* applied NIPS using Polarclean for PSf and CA membranes for desalination.[13] PSf membranes achieved a PWP of 314.5 LMH per bar with 98.1% BSA rejection, while CA membrane exhibited a PWP of 1.5 LMH per bar and NaCl and $MgCl_2$ rejection of 85.1% and 93.2%, respectively.

Hassankiadeh *et al.* prepared PVDF hollow fiber membranes using Polarclean *via* TIPS and NIPS methods.[142] Additives including PVP, poly(methylmethacrylate) (PMMA) and glycerol were incorporated, with PVP enhancing porosity up to 80% and the PWP to 1152 kg m^{-2} h bar. In another study, Ursino *et al.* utilized Polarclean with PVP and PEG to fabricate MFPES hollow fiber membranes *via* NIPS.[163] The highest PWP of 1340 LMH per bar was observed with 18 wt% PES, 40 wt% additives, and a bore fluid composition of H_2O/Polarclean (85/15), due to the larger pore size and thinner membrane.

Zou *et al.* developed a PVDF/PSf membrane using Polarclean and grew an inorganic layer of TiO_2 and Al_2O_3 *in situ* using Pluronic L61 for dispersion.[164] This increased the tensile strength from 1.5 MPa to 9.2 MPa, improved the BSA rejection to ~95%, and enhanced the anti-fouling properties. Later, the same group modified these membranes using tributyl *O*-acetyl citrate as the coating fluid and PEG as a bore fluid for ginseng extraction and water desalination.[165] Although a high ginseng rejection of 99.96% was achieved, the membrane demonstrated low stability, and its applicability for desalination was limited due to its hydrophobic nature. Fluorination and Hyflon modification improved the membrane hydrophobicity, enabling 99.99% salt rejection in direct contact membrane distillation (DCMD) using 0.1 mM sodium dodecyl sulfate (SDS).

Similarly, the chemically recyclable aliphatic polyester (P(4,5-T6GBL)) TFC membrane fabricated by Hardian *et al.* using Polarclean as the casting solvent showed outstanding long-term stability during continuous operation.[166] In a 96 h cross-flow NF test using a 2 g L^{-1} Na_2SO_4 solution at 6 bar and 25 ± 1 °C, the membrane maintained a consistent water flux of 19.5 L m^{-2} h^{-1} and a salt rejection of 98.1%, with negligible variation over time. These results highlight the high durability, mechanical integrity, and chemical resistance of the membrane, validating Polarclean as a green and effective alternative to conventional toxic solvents for fabricating stable NF membranes suitable for prolonged operational use.

Zhu *et al.* fabricated a Janus MHP/PEBA membrane using the green solvent Cyrene™.[167] The membrane exhibited excellent permeate flux stability during 12 h of cross-flow filtration cycles alternating between pure water and secondary wastewater effluent. It also maintained a high removal efficiency (up

to 100% for target pharmaceuticals and personal care products) and over 85% reusability after six adsorption–desorption cycles, with 32% reduction in mechanical strength. These results demonstrate the robust durability and operational stability of the Cyrene™-based membrane under realistic conditions.

7. Polar protic

Polar protic solvents are characterized by their ability to form hydrogen bonds due to the presence of acidic hydrogen atoms (*e.g.*, O–H or N–H groups). These solvents are essential in membrane technology for their high polarity, biocompatibility, and sustainability. Unlike aprotic solvents, they actively participate in hydrogen bonding, which can significantly influence phase separation dynamics and membrane morphology. This section explores Agnique® AMD 3 L, a bio-based polar protic solvent that offers a greener alternative to conventional toxic solvents. Its use in gas and liquid separation membranes highlights its potential to enhance sustainability without compromising membrane performance.

7.1 Agnique® AMD 3 L

Agnique® AMD 3 L, chemically known as *N*,*N*-dimethyl lactamide, is a bio-based solvent derived from lactic acid fermentation. Besides favorable attributes including non-toxicity and biodegradability, high polarity and water solubility make it a promising green alternative to traditional solvents like NMP and DMF, which pose significant environmental and health risks.[168] Agnique® AMD 3 L has been employed as a green solvent in fabricating PES hollow fiber membranes. Studies demonstrated that membranes produced using this solvent exhibited comparable porosity and permeability to those produced with conventional solvents.[169] Replacing hazardous solvents with Agnique® AMD 3 L contributes to a safer working environment and reduces environmental impact. Despite these advantages, several challenges persist in its full integration into membrane manufacturing. Its unique physicochemical properties require adjustments to the fabrication parameters to achieve optimal membrane morphology and performance. Additionally, its higher hydrogen bonding capacity can alter the phase separation behavior, potentially affecting the pore structure and distribution during membrane fabrication.[35] The relatively high boiling point of Agnique® AMD 3 L may also complicate solvent removal and necessitate tighter process control.[57] Addressing these challenges requires further research aimed at optimizing membrane fabrication protocols to fully leverage the benefits of this green solvent in sustainable membrane technology.

7.2 Applications of polar protic-based solvents in liquid separation

To date, the applications of Agnique® AMD 3 L in membrane fabrication have been limited but promising, with notable examples including CA hollow fiber membranes for forward osmosis (FO),[168] PES hollow fiber membranes for liquid–liquid separation,[169] and PESU flat sheet membranes for ultrafiltration.[35] The CA hollow fiber membranes fabricated using Agnique® AMD 3 L exhibited excellent mechanical stability, characterized by dense outer surfaces and porous, sponge-like structures that minimized macrovoid formation. These membranes achieved a MWCO of less than 100 g mol^{-1}, with high rejections for anionic dyes (>99%) and sulfate ions (>90%), attributed to the hydrated size and negative charge of these solutes (Fig. 13(a)). In FO testing, the membranes showed competitive water fluxes from 2.0 to 6.2 LMH and low reverse salt fluxes, particularly when annealed under humid air conditions, which enhanced the performance without compromising structural integrity.[168]

Agnique® AMD 3 L also showed great potential as a green solvent in the fabrication of PES hollow fiber membranes *via* the NIPS process. Compared to the conventional solvent *N*-ethyl-2-pyrrolidone (NEP), Agnique® AMD 3 L exhibited a higher affinity

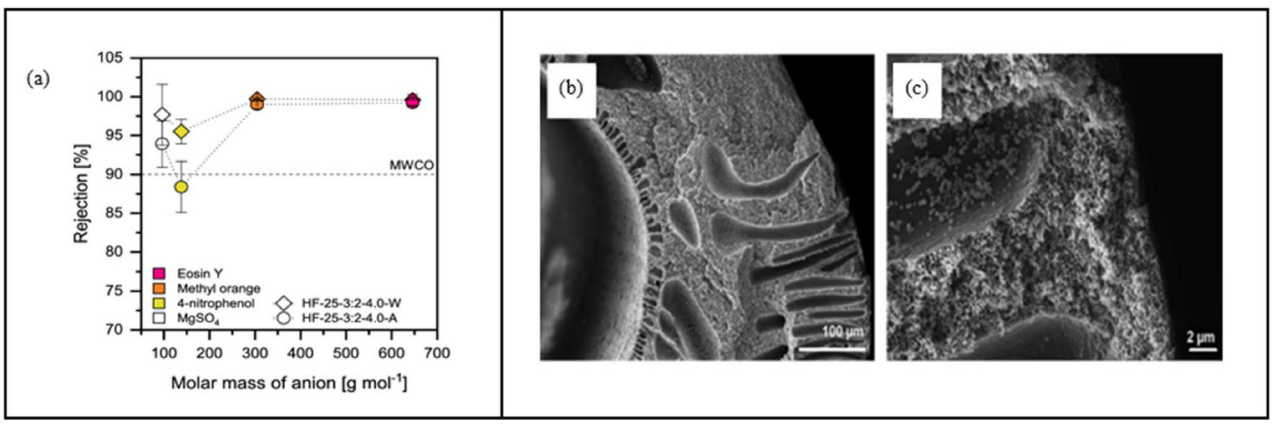

Fig. 13 (a) Rejection of anionic dyes and magnesium sulfate by CA hollow fiber membranes prepared with Agnique® AMD 3 L. Reproduced from ref. 168 with permission from American Chemical Society, copyright 2023. (b) and (c) SEM images of the cross-sectional morphology of PES hollow fiber membranes prepared with Agnique® AMD 3 L. Reproduced from ref. 169 with permission from Wiley Periodicals LLC, copyright 2021.

for water and a lower affinity for PES, leading to faster phase separation.[169] This resulted in membranes with larger pore sizes and higher porosity, which contributed to a PWP of up to 406.9 kg m^{-2} h^{-1} bar^{-1}, attributed to their open and sponge-like structures (Fig. 13(b) and (c)). For PESU ultrafiltration membranes, Agnique® AMD 3 L enabled the fabrication of membranes with hydraulic permeability up to 610 kg m^{-2} h^{-1} bar^{-1} and MWCO values up to 20 kDa, comparable to membranes prepared using conventional solvents like NMP and DMAc.[35] Additionally, membranes fabricated with Agnique® AMD 3 L retained significantly lower levels of residual solvent, thereby reducing the need for extensive post-treatment and enhancing safety for applications in drinking water purification and haemodialysis.

8. Organic salts

Organic salts, particularly ionic liquids (ILs) and deep eutectic solvents (DESs), have emerged as innovative and sustainable alternatives to conventional solvents in separation processes. Their unique physicochemical properties, such as low volatility, high thermal stability, and tunable solvation behaviour, make them highly attractive for gas and liquid separation applications. ILs composed of organic cations and anions, offer exceptional versatility due to their customizable structures. ILs offer significant advantages in fabricating CO_2 capture membranes due to their strong affinity for CO_2 and their ability to tailor the membrane morphology, enabling the formation of optimal pore structures for enhanced gas separation performance.[170] In contrast, DESs are formed through hydrogen-bonding interactions between hydrogen bond donors (HBDs) and hydrogen bond acceptors (HBAs). They offer a greener and more cost-effective synthesis route due to their lower raw material costs, ease of synthesis, and minimal purification requirements.[171] Over the past decade, advancements in bio-derived ILs and natural deep eutectic solvents (NADESs) have further enhanced their environmental compatibility. This section explores the properties, synthesis, and applications of ILs and DESs in gas and liquid separation technologies, highlighting their potential to improve efficiency, selectivity, and sustainability in industrial processes.

8.1 Ionic liquids (ILs)

ILs are low melting organic salts composed of various combinations of organic cations and anions. Their physical and chemical properties can be precisely tuned by selecting and combining specific cation–anion pairs. At an early stage when ILs were introduced as functional solvents, ILs such as those based on imidazolium or pyridinium cations and halogenoaluminate(III) anions were highly sensitive to air and moisture, which limited their practical applications. Over the years, second and third generation ILs have been developed with improved characteristics including enhanced air and water stability, low toxicity and greater biodegradability.[172] In the past 10 years, research has increasingly focused on the development of greener ILs derived from renewable feedstocks to support a closed-loop biorefinery approach. Examples of such bio-based ILs include those synthesized from proteins, polysaccharides, sugars, and lignin, as illustrated in Fig. 14. Numerous reviews have extensively discussed the application of ILs across diverse fields, including energy storage, green catalysis, CO_2 capture, biomass processing, pharmaceuticals, and advanced materials. Hulsbosch *et al.* conducted a comprehensive review of ILs synthesized from green precursors.[173] These include cationic species such as quaternary ammonium salts, amino acids, and ester derivatives and anion species such as halides, phosphates, natural carboxylates, and sugar analogs. Valorizing the bio-derived ILs over conventional ILs offers environmental advantages, including reduced ecological impact and improved recyclability. Key application areas include solvent extraction, gas absorption, membrane gas separation, and electrochemical systems. Besides, ILs have been widely applied as safe electrolytes in batteries and fuel cells due to their high conductivity, low flammability, and high regeneration ability.[174] Conventional ILs typically capture CO_2 *via* physical absorption, relying on weak dipole–dipole interactions, van der Waals forces, and hydrogen bonding. Nonetheless, these interactions are often insufficient under flue gas conditions with low CO_2 partial pressures. To address this, task-specific ionic liquids (TILs) have been developed with functional groups such as amino acids, imidazoles, or phenols that enable chemical absorption of CO_2 through carbamate formation, thereby enhancing capture efficiency.[175]

8.2 Deep eutectic solvents (DESs)

Deep eutectic solvents (DESs) are formed by combining a HBD and HBA through hydrogen bond interactions. They remain in a liquid state at temperatures below 100 °C and possess melting points lower than those of their individual components.[176] The synthesis process is simple as HBDs and HBAs are first mixed by grinding, followed by heating within the range of 50–100 °C until a homogeneous solution is obtained. Recently, new synthesis methods such as ultrasound-assisted extraction (UAE) and microwave-assisted extraction (MAE) were introduced. However, the most established and straightforward approach remains traditional heating and stirring, owing to its simplicity and low cost.[177] DESs exhibit properties similar to those of ILs, including high thermal and chemical stability, non-flammability, and negligible vapor pressures. However, they offer additional advantages such as biodegradable, lower toxicity, reduced combustibility, and easier synthesis. As such, DESs are highly recommended for long-term applications. For example, DESs composed of choline chloride, propanediol, and sugars have been reported to be biodegradable when prepared with sugars, glycerol, and oxalic acid as HBDs, showing non-toxic effects and non-environment impact.[178] Recently, a new class of DES, NADESs, was developed from natural sources such as plants, animals, and microorganisms. NADESs are considered more environmentally friendly and greener alternatives to conventional DESs. They are typically composed of proteins and plant-based metabolites such as sugars, ammonium salts, amino acids, and organic acids, making them renewable and highly biocompatible. Different from ILs, NADESs possess unique features such as stability, biodegradability, and re-

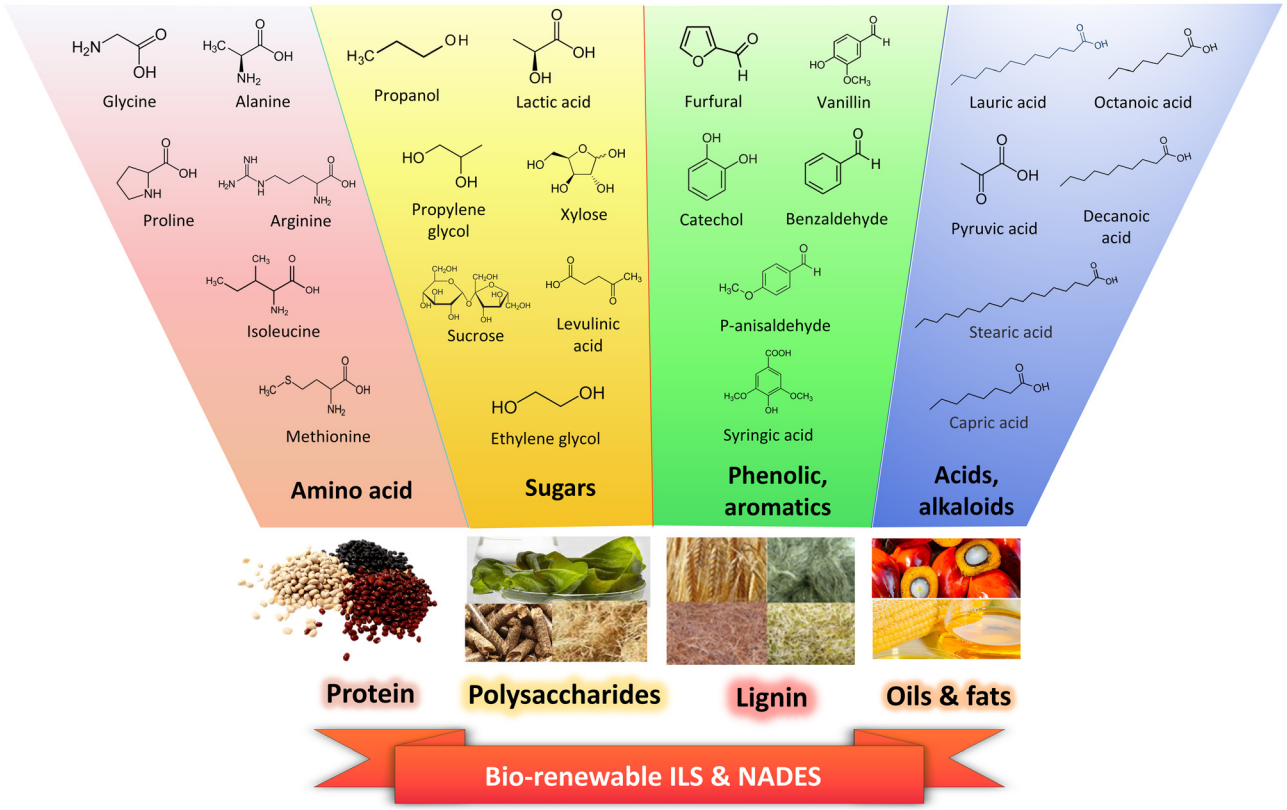

Fig. 14 Renewable resource classes used in the synthesis of ILs and NADESs.

usability, making them suitable for various applications including extraction, chromatographic media, gas separation, and biomedical uses. In CO_2 capture, many NADESs containing CO_2-philic functional groups including amines, carbonyls, ethers and fluorinated groups have been employed for both absorption and adsorption processes. These have demonstrated significant improvements in carbon capture kinetics and CO_2 capture capacity.[179]

8.3 Applications of organic salt-based solvents in gas separation

Due to the low volatility and non-flammability of ionic liquids, ILs have been used as alternatives to conventional organic solvents in polymer synthesis. One study demonstrated the application of 1-ethyl-3-methylimidazolium trifluoromethane sulfonate in the free radical polymerization of methyl methacrylate and acrylonitrile, resulting in high molecular weight PMMA and PAN.[180] In atom transfer radical polymerization, 1-methyl-imidazolium acetate, 1-methylimidazolium propionate, and 1-methylimidazolium butyrate showed excellent performance in the polymerization of methyl methacrylate using ethyl 2-bromoisobutyrate/CuBr as the initiating system. A strong correlation was observed between the polymerization rate and the length of the substituted anion groups in the ILs.[181]

Regarding support synthesis, Ziobrowski and Rotkegel impregnated 1-ethyl-3-methylimidazolium acetate ([EMIM][Ac]) in the nanopores of ceramic supports in commercial PDMS and MF membranes for CO_2/N_2 separation.[182] The ceramic-supported PDMS coated with [EMIM][Ac] surpassed the Robeson upper bound, exhibiting a superior selectivity of up to 152.0, outperforming the [EMIM][Ac]/PDMS membrane prepared *via* the soaking method. In contrast, the MF membrane impregnated with IL demonstrated significantly lower separation performance due to insufficient pore coverage, leading to IL loss.

ILs have been used not only as solvents but also as raw materials and chemical or physical modifiers in membrane fabrication. Chen *et al.* reported that dissolving various polymers (*e.g.*, PES, PVDF, polyamide) in ILs to fabricate ionic liquid–polymer membranes (ILPMs) addressed the stability issue encountered in supported ionic liquid membranes (SILMs).[183] Embedding ILs into the polymer matrix enhances membrane permeability and selectivity, especially when functionalized ILs are used. Additionally, membranes prepared through physical blending or chemical grafting of ILs with polymers from free-standing and mechanically robust films do not require additional support layers. Interestingly, Zou *et al.* found that incorporating ILs into PES altered the phase separation mechanism, creating porous morphologies that were typically unattainable using conventional organic solvents.[25]

Shafie *et al.* highlighted the potential of ILs in polymeric membranes for CO_2 capture owing to their high CO_2 affinity.[184] Incorporating ILs increases the free fractional

volume (FFV) of the membrane, improving gas diffusivity and creating more sorption sites. Higher IL loading enhances CO_2 solubility by increasing the solubility coefficient. Mannan *et al.* reported superior membrane performance when 1-ethyl-3-methyl imidazolium bis(trifluoromethylsulfonyl)imide ([EMIM][Tf_2N]) was incorporated into PES.[185] A membrane with 50% [EMIM][Tf_2N] loading exhibited a CO_2/CH_4 selectivity of 49.0 and CO_2 permeability of 355.7 barrer, validating the benefits of IL incorporation for gas separation.

Shafie *et al.* also discussed the incorporation of ILs in MMMs, where ILs enhanced the gas separation efficiency through improved interactions between the polymer and inorganic phase.[184] ILs contribute additional FFV, thereby increasing membrane permeability. The fabrication of IL MMMs involves more steps than conventional polymeric membranes, including dispersing inorganic particles in a solvent, sonication, priming and stirring, casting the dope solution, and drying.[156] Fig. 11(d) illustrates the schematic process for preparing IL MMMs. Cardoso *et al.* investigated membranes containing 10 to 40 wt% [EMIM][Tf_2N] in PES/SAPO-34 MMMs.[186] The optimum membrane performance was observed at 20 wt% IL loading, yielding a CO_2/N_2 selectivity of 39.4 and CO_2 permeability of 2.1 barrer. Increasing the IL loading from 10 to 20 wt% enhanced the selectivity by reducing the free volume available for N_2, thus favoring CO_2 transport. Nevertheless, further increases in IL concentration led to a decline in selectivity, attributed to increased polymer chain mobility, which raised the permeability of both CO_2 and N_2. The findings confirm that the incorporation of ILs into MMMs can significantly enhance the membrane performance for gas separation.

Shah Buddin *et al.* explored two modification approaches for ZIF-L-based PES MMMs using 1-butyl-3-methylimidazolium tetrafluoroborate ([BMIM][BF_4]) IL *via* (i) pre-modification, whereby ZIF-L was treated with the IL before incorporation into PES, and (ii) post-modification, where the IL was introduced after the formation of PES/ZIF-L MMMs.[187] The pre-modified PES/ZIF-L MMM exhibited an improved gas separation performance at 0.75 wt% IL loading with the CO_2 permeability increasing by 867%, and CO_2/N_2 and CO_2/CH_4 selectivities of 30.1 and 21.8, respectively. This is attributed to reduced interfacial voids and a strong affinity between the IL and CO_2. In contrast, post-modification led to disrupted polymer chains, enhancing permeability but reducing selectivity.

Patil *et al.* investigated the CO_2/CH_4 separation performance of SILMs composed of Pebax-1657 and [BMIM][Ac].[188] Due to the higher interaction energy of CO_2 with [BMIM][Ac] compared to CH_4, CO_2-dominated permeation was observed. Among membranes containing 0–20 wt% IL, the Pebax membrane with 20 wt% IL demonstrated a superior separation performance in both single and mixed gas permeation tests. At 2.5 bar during mixed gas testing, this membrane exhibited a 52% increase in CO_2 permeability and a 78% improvement in CO_2/CH_4 selectivity over pristine Pebax, approaching the Robeson upper bound (Fig. 15(a) and (b)). However, the poor miscibility of ILs in the polymer matrix at high loadings

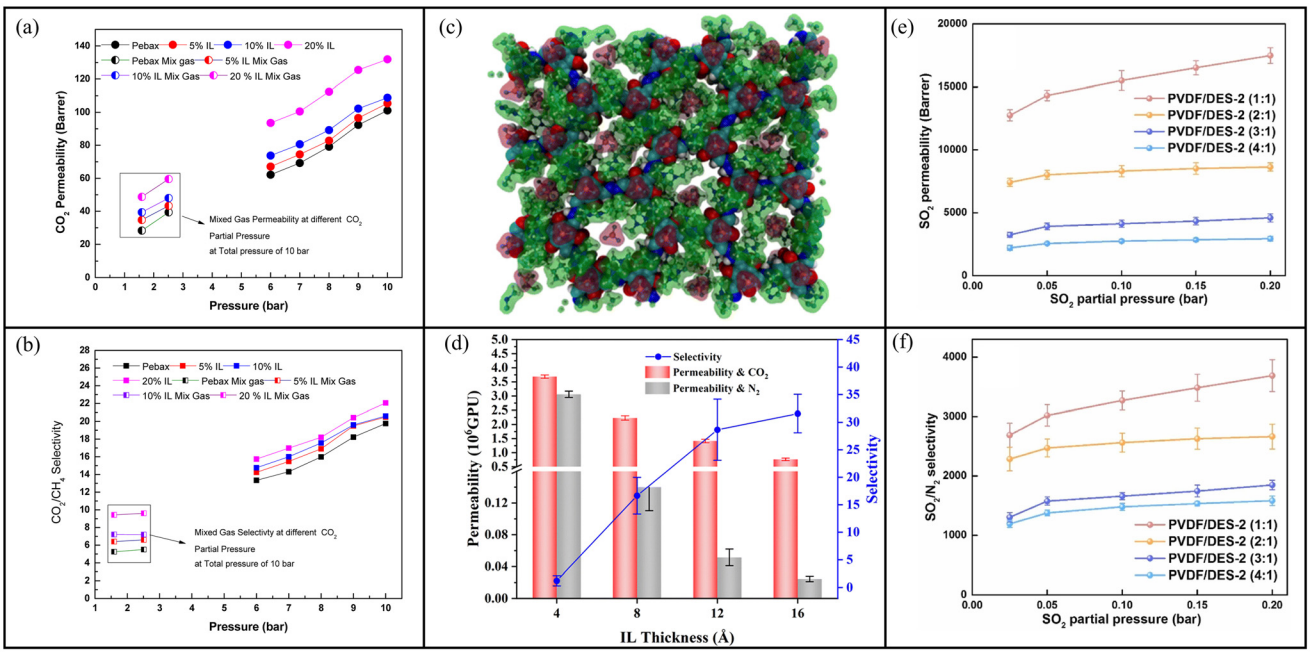

Fig. 15 (a) CO_2 permeability and (b) CO_2/CH_4 selectivity of [BMIM][Ac]/Pebax-1657 SILMs. Reproduced from ref. 188 with permission from Elsevier B.V., copyright 2023. (c) Top view of the bilayer COF membrane incorporating [BMIM][BF_4], (d) CO_2/N_2 permeability and selectivity as a function of IL thickness. Reproduced from ref. 192 with permission from the Royal Society of Chemistry, copyright 2022. (e) SO_2 permeability and (f) SO_2/N_2 selectivity of PVDF/DES blended membranes. Reproduced from ref. 193 with permission from Elsevier B.V., copyright 2023.

adversely affected the mechanical stability due to structural inhomogeneity.[189–191]

A 2D-COF-based SILM was developed for CO_2/N_2 separation, exceeding the Robeson upper bound.[192] The membrane utilized [BMIM][BF_4] as the IL and NUS-2 as the covalent organic framework (COF) (Fig. 15(c)). The [BMIM][BF_4] layer imparted a gating effect, enabling selective CO_2 adsorption and permeation while hindering N_2 transport. Among membranes with varying IL thicknesses (*e.g.*, 4, 8, 12, and 16 Å), the bilayer COF-SILM with an 8 Å IL exhibited optimal performance (Fig. 15(d)). Thicker IL layers increased the gas transport resistance, reducing CO_2 permeability, while monolayer COFs and 4 Å ILs failed to sufficiently expose COF pores, resulting in lower selectivity. The optimized membrane thus offers promising potential for efficient CO_2/N_2 separation.

Zhang *et al.* further explored PVDF membranes incorporating a DES composed of 1-butyl-3-methyl-imidazolium bromide ([BMIM]Br) and diethylene glycol (DEG) for SO_2 separation.[193] The inclusion of the DES significantly enhanced the $SO_2/CO_2/N_2$ separation performance (Fig. 15(e) and (f)). Compared to pristine PVDF membranes with SO_2 permeability of 3.2 barrer, the PVDF/DES (1 : 1) membrane achieved a remarkable SO_2 permeability of 17 480 barrer. Moreover, the [BMIM]Br : DEG molar ratio influenced selectivity, with a 2 : 1 ratio yielding outstanding SO_2/N_2 and SO_2/CO_2 selectivity of 8109 and 344, respectively. These results confirm the high potential of PVDF/DES membranes for selective SO_2 separation.

Saif-ur-Rehman *et al.* explored the feasibility of incorporating DESs to functionalize fillers when fabricating DES-SBA-15/PSf MMMs for CO_2 separation.[194] The SBA-15 fillers were functionalized through a solvent evaporation technique using a DES synthesized from choline chloride and decanoic acid. Among the membranes with DES-SBA-15 loadings ranging from 0 to 20 wt%, the 20 wt% DES-SBA-15 MMM demonstrated the highest CO_2/CH_4 and CO_2/N_2 separation performance; this was attributed to increased porosity. This membrane achieved a CO_2 permeability of 22.3 barrer with CO_2/CH_4 and CO_2/N_2 selectivities of 57.1 and 59.9, respectively. The improved performance was attributed to the DES-functionalized SBA-15 introducing uniformly distributed small pores and enhancing CO_2-specific interactions with the PSf matrix.

In a related study, Saif-ur-Rehman *et al.* reported enhanced CO_2 separation using DES–ceria as fillers in PSf MMMs, compared to a pristine PSf membrane.[195] The DES–ceria nanoparticles were synthesized by mixing cerium oxide with a DES at an 8 : 1 weight ratio in ethanol, followed by solvent evaporation. The membrane with 8 wt% DES–ceria achieved the best mixed-gas separation performance among the 0–8 wt% loadings, with CO_2 permeability of 16.3 barrer and CO_2/CH_4 and CO_2/N_2 selectivities of 35.4 and 39.3, respectively, approaching the Robeson 2008 upper bound. The enhancement was attributed to the interactions between the amine groups and carboxyl groups in the DES–ceria and CO_2 molecules.

Craveiro *et al.* explored supported liquid membranes (SLMs) (Fig. 11(c)) using polytetrafluoroethylene (PTFE) supports and DES formulations comprising choline chloride (ChCl) as a HBA and urea, glycerol, ethylene glycol, or oxalic acid as HBDs.[196] Carbonic anhydrase (CA*), an enzyme that catalyzed the conversion of CO_2 into bicarbonate, was incorporated to enhance CO_2 sorption. However, CA* reduced CO_2 solubility in ChCl : glycerol, ChCl : ethylene glycol, and ChCl : oxalic acid DESs due to their high acidity. In constrast, ChCl : urea stabilized CA* *via* hydrogen bonding with the enzyme surface, enhancing both its stability and CO_2 solubility. Overall, the DES SLMs generally increased CO_2 permeability, although gas selectivity improvements were limited; only ChCl : oxalic acid showed enhanced selectivity after CA* incorporation. Notably, the ChCl : urea PTFE membrane without CA* surpassed the Robeson upper bound for CO_2/CH_4 separation, achieving a selectivity of around 90 and CO_2 permeability of 100 barrer, indicating strong potential for gas separation applications.

In another study, Saeed *et al.* incorporated DESs derived from betaine as the HBA with glycerol, ethylene glycol, and urea as the HBDs into microporous PVDF membranes.[197] Betaine was selected for its sustainability, low toxicity, and biodegradability. A 1 : 3 molar ratio of betaine : urea exhibited enhanced CO_2/CH_4 separation, with a CO_2 permeability of 35.6 barrer and a selectivity of 57.5, outperforming the betaine : glycerol system. This improvement was primarily attributed to the strong CO_2 affinity of the betaine : urea DES. Both betaine : urea and betaine : glycerol SLMs exhibited thermal stability up to 200 °C because of strong hydrogen bonding between the HBA and HBD. These DESs offer a promising, greener alternative to conventional ILs in SLMs, with performances approaching the Robeson upper bound.

8.4 Applications of organic salt-based solvents in liquid separation

Pragmatically, DESs have been employed in membrane fabrication to enhance their permeability and anti-fouling properties.[25] Shahabi *et al.* reported that the introduction of 1% DES into polyamide membranes led to a 27% improvement in water permeability and an approximately 3% increase in NaCl rejection compared to the pristine membrane for desalination.[198] These enhancements were attributed to increased membrane hydrophilicity, resulting from hydrogen bonding interactions between the amine groups in the polyamide and the N–H, –OH, and C═O groups in the DESs. However, DES-modified membranes also exhibited smoother surfaces, which reduced the effective filtration area and water flux. In other work, Russo *et al.* successfully incorporated benzyl-trimethylammonium mesylate/*p*-toluenesulphonic acid monohydrate (PTSA/TBnA MsO) DES and phenyl acetic acid/trimethyl glycine (PhAA/TMG) NADES as organic solvents for PVDF membrane fabrication.[199] For PAN membranes, sulfobetaine-based DESs were used, including (1*S*)-(+)-10-camphorsulfonic acid/(3-(1-methyl-1*H*-imidazole-3-ium-3-yl)propane-1-sulfonate) ((+)CSA/SB3-MIM) and (1*S*)-(+)-10-camphorsulfonic acid/3-(*N*,*N*-dimethybutylammonio)propane-1-sulfonate ((+)CSA/SB3-4). Due to the inherently high viscosity of DESs, co-solvents such as water and polar aprotic solvents (*e.g.*, TEP) were employed

to facilitate membrane casting by reducing the solution viscosity. Among the PVDF membranes fabricated, the one prepared using PhAA/TMG as the DES and TEP as a co-solvent exhibited the highest PWP of 3243 LMH per bar. Additionally, the membrane synthesized using PTSA/TBnA MsO as the DES and TEP as the co-solvent showed the highest methylene blue rejection of 76%, which was ascribed to its variable pore size distribution.

ILs and DESs offer tunable physicochemical properties and have shown significant promise in membrane separation processes. However, their practical implementation in continuous or large-scale operations requires several key challenges to be addressed. Recyclability and recovery of ILs and DESs remain active areas of research. ILs, especially those with a low vapor pressure, can be recovered through vacuum distillation, solvent extraction, or membrane-based separation while hydrophilic ILs may also be recovered using aqueous two-phase systems (ATPS).[200] For DESs, membrane filtration has emerged as a non-thermal recovery method, often facilitated by dilution with water, ethanol, or acetone to reduce viscosity and improve processability.[201] High viscosity is a current limitation for both ILs and DESs, as it adversely affects mass transfer and permeation rates in membrane systems. Strategies such as dilution or the use of ultrafiltration configurations can help mitigate these issues and enhance separation efficiency.[202] The diffusion behaviour of solutes in IL or DES systems is highly dependent on solvent viscosity and solute–solvent interactions, which directly influence transport dynamics through the membrane matrix.[203] In terms of leaching and retention, ILs typically exhibit strong retention within membrane pores due to their negligible vapor pressure; this enhances membrane stability and enables selective separation *via* tailored IL–solute interactions.[204] On the other hand, DESs are increasingly used as solvents, additives, or pore formers during membrane fabrication, modifying the membrane structure and affecting properties such as porosity and pore size. DES-based SLMs have also shown promise for gas separation, although stability and long-term performance remain critical concerns.[205] Overall, while ILs and DESs demonstrate strong potential in lab-scale applications, further studies are required to validate their stability, recyclability, and transport behaviour under industrial or continuous operation conditions.

9. Expanding the use of green solvents: vegetable oils in emulsion liquid membranes (ELMs)

While earlier sections of this review focus primarily on green solvents for polymeric membrane fabrication, vegetable oils also represent a promising class of green solvents for emulsion liquid membranes (ELMs). Incorporating bio-based oils into ELM systems broadens the scope of green-solvent applications, contributing to sustainable liquid–liquid separation technologies. However, their applicability in conventional membrane casting (*e.g.*, *via* phase inversion) is limited, as these oils generally cannot dissolve polymers such as PVDF, PES, or PSf, making them unsuitable as primary solvents. Nevertheless, research has explored their use as additives or pore formers in polymer blends, where they can influence membrane morphology or hydrophobicity. Conventional petroleum-based diluents such as kerosene pose significant environmental and safety concerns due to their toxicity, flammability, volatility, and non-renewable nature. In contrast, vegetable oils such as palm oil, rice bran oil, and sunflower oil offer eco-friendly alternatives with high thermal stability, low volatility, and excellent solvation capabilities. These properties not only improve the performance of ELMs in applications such as heavy metal removal, organic compound extraction, and wastewater treatment, but also align with the principles of green chemistry. This section evaluates the physicochemical properties, advantages, and specific applications of these oils in ELM systems, highlighting their potential to replace conventional solvents in liquid separation processes.

9.1 Palm oil

Palm oil is among the most commonly utilized vegetable oils in ELM fabrication, serving as a renewable and sustainable alternative to traditional petroleum-based diluents.[206] Palm oil is non-toxic, biodegradable, non-volatile, and non-flammable, featuring a high flash point, low dielectric constant, and low melting point. Notably, palm oil lacks a TLV-TWA value, indicating minimal occupational health risks.[207] Moreover, palm oil is readily available, cost-effective, and has high global productivity, making it an attractive green solvent. Palm oil has been effectively applied in the extraction of heavy metals and organic compounds such as succinic acid. It also shows strong potential for phenol extraction due its ability to form hydrogen bonds or other intermolecular interactions between phenol and triglycerides in the oil, resulting in phenol–triglyceride complex formation.[208] The separation process involves both partitioning (dissolution) and complexation mechanisms, facilitated by the hydrophobic characteristics of palm oil and its high viscosity, which enhances emulsion stability.[209]

9.2 Rice bran oil

Rice bran oil (RBO) is the second most viscous vegetable oil after palm oil and contains approximately 24% palmitic acid (C16:0), 42% oleic acid (C18:2), and 34% linoleic acid (C18:1), which closely aligns with the fatty acid ratio of 1 : 1.5 : 1 (saturated:monounsaturated:polyunsaturated) recommended by the World Health Organization (WHO).[210,211] Owing to its high viscosity, RBO significantly enhances the stability of green emulsion liquid membranes (GELMs), exhibiting the highest static stability of 120 min among various tested vegetable oils, including olive, groundnut, soyabean, sunflower, coconut and mustard oils.[212] This superior static stability allows for extended extraction times and promotes efficient

separation between the membrane and internal phases during the emulsion process. Derived from the inner rice husk, RBO offers several favorable attributes such as being non-toxic, cost-effective, readily available, and possessing a high smoke point. Physically, RBO has a density of 910 g L^{-1}, a refractive index of 1.467, and an absolute viscosity of 59.3 cP.[211] Additionally, it naturally contains bioactive compounds such as oryzanol, polycosanol, and ferulic acid, which act as surface-active agents. These molecules reduce interfacial tension between the aqueous and oil phases, prevent droplet coalescence, and thereby contribute to enhanced emulsion stability.[210–212]

9.3 Sunflower oil

Sunflower oil is emerging as a viable green solvent for ELM applications. It is biodegradable, renewable, cost effective and has low toxicity.[213,214] In ELM fabrication, sunflower oil can serve as the membrane phase, which is the organic phase. It can create stable emulsions with both internal and external aqueous phases; this is crucial for determining ELM efficiency. It functions as a selective barrier, facilitating the transport of desired solutes while excluding undesired components. Moreover, sunflower oil is capable of dissolving specific carriers including compounds that aid in the selective transport of substances and additives that enhance the performance of the ELM.[215,216] Sunflower oil-based ELMs have demonstrated efficacy in the removal of various contaminants, including heavy metals such as chromium[217–219] and copper[220] from industrial wastewater, as well as the extraction of pharmaceutical compounds such as the antibiotic vancomycin,[216] and other organics like lignosulfonate.[221] These applications underscore the potential of sunflower oil in developing sustainable and effective liquid separation technologies.

9.4 Applications of oil-based solvents in liquid separation

ELM technology is an advanced separation method that synergistically combines the principles of liquid–liquid extraction and membrane technology. The system typically involves the formation of a double emulsion, either water-in-oil-in-water (W/O/W) or oil-in-water-in-oil (O/W/O), where a primary emulsion is dispersed within a continuous phase. The membrane phase, often an organic solvent, acts as a barrier that selectively transports target solutes from the feed phase to the receiving phase. ELM is widely used for the extraction and recovery of metals, organic compounds, and biomolecules due to its high efficiency, selectivity, and suitability for treating dilute solutions.[222,223]

Palm oil demonstrated excellent performance as a green and sustainable membrane phase in ELM applications. In a study focused on Cr(VI) removal from wastewater, palm oil was used with Span 80 (*e.g.*, as a surfactant) and bis(2-ethylhexyl) phosphate (*e.g.*, as a carrier). The system achieved effective emulsion stabilization and high Cr(VI) removal efficiency. Optimal operating conditions included a TOMAC concentration of 0.4 M, NaOH stripping agent at 0.3 M, and agitation speed of 8000 rpm, which led to substantial Cr(VI) recovery. The use of palm oil not only enhanced the stability and efficiency of the ELM system but also aligned with eco-friendly practices due to its biodegradability and low toxicity.[224] In a continuous emulsion liquid membrane (CELM) process for phenol recovery, palm oil combined with Span 80 (*e.g.*, as a surfactant) and sodium hydroxide (*e.g.*, as a stripping agent) also exhibited outstanding performance. Under optimal conditions, including a rotational speed of 527 rpm, a treat ratio of 1 : 4, and a retention time of 2.6 min, the system achieved nearly 100% phenol recovery and a sevenfold (*e.g.*, 2100 ppm) enrichment in the internal phase.[225] These findings emphasize the efficacy and sustainability of palm oil as a replacement for conventional solvents in ELM applications, particularly in effluent treatment.

RBO has demonstrated exceptional potential as a green and sustainable diluent in ELM systems. In combination with Span 80 (*e.g.*, as a surfactant) and NaOH (*e.g.*, as a stripping agent), RBO achieved a dynamic emulsion stability of up to 150 min with less than 1% membrane breakage. Optimal conditions, including an emulsification speed of 2100 rpm, 2% Span 80 concentration, and a treat ratio of 1 : 3.5, ensured stable emulsion formation and enhanced performance. Additionally, RBO has proved effective as a green solvent in the green emulsion ionic liquid membrane (GEILM) system for the extraction of lactic acid (LA), achieving a 90% extraction efficiency and a static emulsion stability of 90 min.[211] Owing to its natural composition, biodegradability, and low toxicity, RBO is considered a cost-effective and environmentally friendly solvent for ELM-based separations. These attributes make RBO particularly suitable for the sustainable extraction of low-concentration solutes in wastewater treatment and resource recovery.

Sunflower oil is another promising candidate for use as a green solvent in GELM systems. It has been employed effectively for the extraction of Cu(II) ions from aqueous solutions, achieving a Cu(II) extraction efficiency above 94% with stable emulsion durations of up to 130 min.[220] Furthermore, sunflower oil has been explored for Cr(VI) recovery using ELMS, as depicted in Fig. 16(a). A study by Anarakdim *et al.* highlighted that sunflower oil, combined with surfactants such as polyglycerol polyricinoleate and Tween 80, could form stable water-in-oil emulsions with over 99% extraction efficiencies over a Cr(VI) concentration range of 0.043 to 50 ppm. The emulsions were efficiently demulsified using heat treatment at 80 °C for 2 h, achieving a demulsification efficiency of 96%. Importantly, DSC and FTIR analyses confirmed that the recovered oil retained its quality and could be reused up to four times without significant degradation or loss of performance.[217] These results emphasized the potential of sunflower oil as a sustainable and cost-effective substitute for traditional petroleum-based solvents in ELM processes. Its biodegradability, renewability, and capacity for reuse offer both environmental and economic advantages in heavy metal remediation from industrial wastewater.

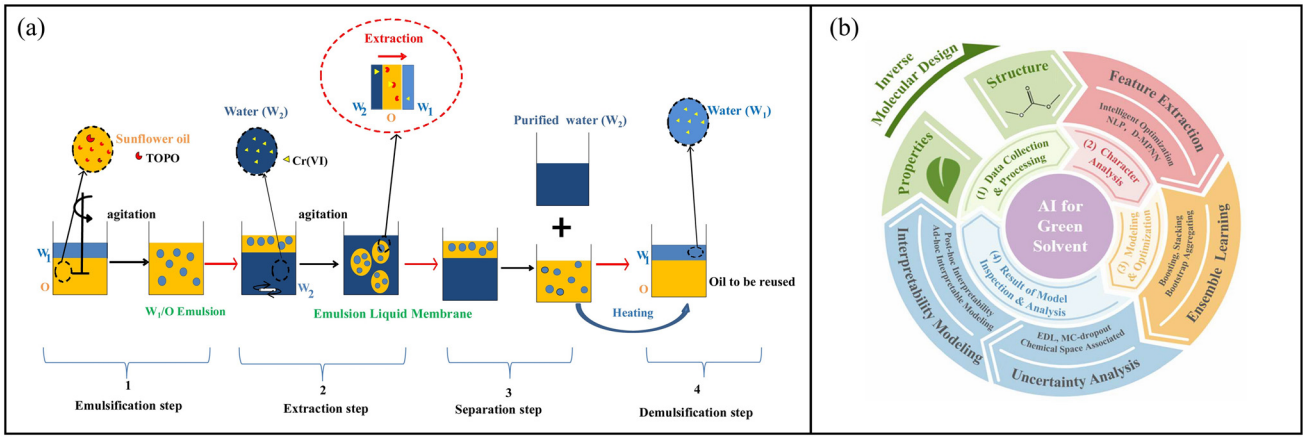

Fig. 16 (a) Schematic diagram illustrating Cr(VI) extraction using an ELM system with oil recovery *via* heat-induced demulsification. Reproduced from ref. 217 with permission from Elsevier B.V., copyright 2020. (b) Overview of AI-assisted solvent design strategies, covering the entire workflow from data collection to inverse molecular design, reproduced from ref. 226 with permission from American Chemical Society, copyright 2023.

10. Artificial intelligence (AI) tools for green membrane preparation

Computational approaches such as quantitative structure–property relationship (QSPR) models have been employed to screen suitable green solvents with high accuracy and efficiency. Wen *et al.* demonstrated the effectiveness of AI-driven frameworks for the design of green solvents, highlighting strategies to integrate computational methods into solvent innovation.[226] They summarized the overall intensification methods for AI-assisted green solvent design, as illustrated in Fig. 16(b).

Wang *et al.* developed a universal deep-learning model, DeepH, that predicted density functional theory (DFT) Hamiltonians for a wide range of materials with high accuracy (mean absolute error: 2.2 meV).[227] Their approach utilizes equivariant neural networks trained on a large database of materials containing 12 062 structures to simulate electronic properties, while overcoming the "gauge problem" in DFT through a novel gauge-invariant loss function. This enables efficient prediction of material behaviors, including solubility and intermolecular interactions, without the need for costly quantum computations. DeepH optimizes green solvent selection for membrane fabrication by simulating solvent–polymer affinity.

Graph neural networks (GNNs), revealed to be a powerful tool for atomic-level insights, are specifically designed for graph-structured data, where nodes represent entities (*e.g.*, atoms or molecules) and edges represent relationships (*e.g.*, chemical bonds). Unlike traditional methods, GNNs automatically capture complex interactions without extensive feature engineering, making them ideal for molecular system modeling. For instance, Ignacz *et al.* applied GNNs to analyze solute–solvent–membrane interactions in OSN, revealing how functional groups and molecular substructures influence membrane performance.[228] In addition, AI-based optimization techniques have proved useful in membrane design and performance evaluation. Models such as genetic algorithm (GA), particle swarm optimization (PSO), and Bayesian optimization have been applied to optimize membrane configurations, operating parameters, and sustainability metrics.[229] AI has also been proposed for use in both computational and experimental scientific discovery, where autonomous AI-driven experiments can replace traditional testing in membrane fabrication for water purification and gas separation.[230]

To identify suitable solvents for polymer dissolution, Chandrasekaran and co-workers compiled data on 4500 polymers and their corresponding solvents and non-solvents to train a deep neural network binary classifier.[231] In their approach, polymers were represented using the simplified molecular-input line-entry system (SMILES), while solvent descriptors were used as additional inputs. The model predicts whether a solvent can dissolve a given polymer by evaluating the absolute difference in Hildebrand solubility parameters between the polymer and solvent, classifying solvents with

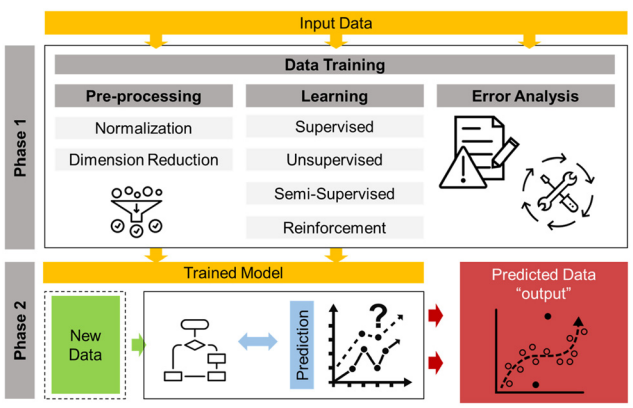

Fig. 17 General overview of the data-driven algorithm execution process. Reproduced from ref. 236 with permission from Elsevier B.V., copyright 2023.

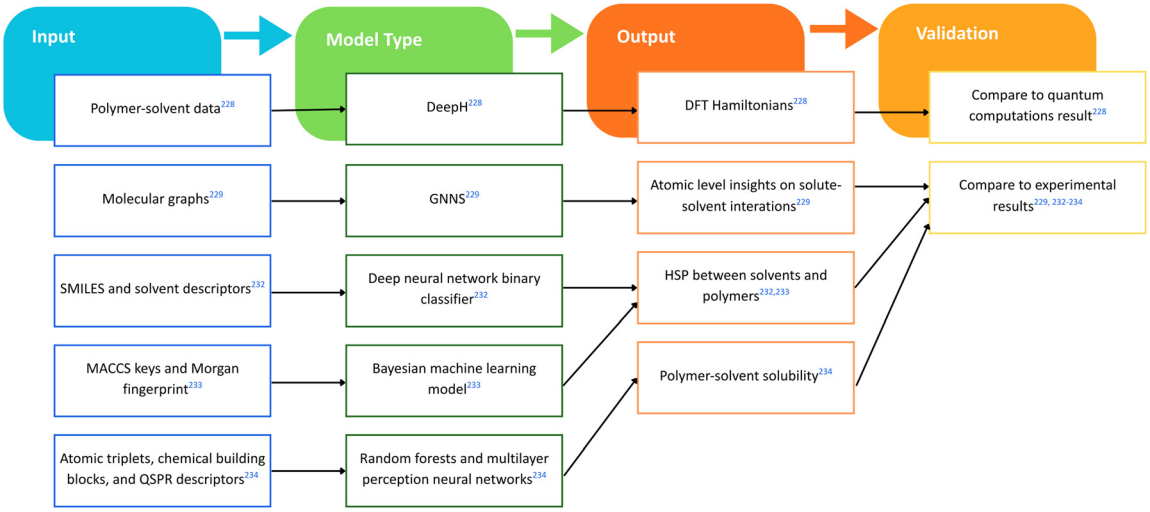

Fig. 18 Schematic representation of the AI workflow for selecting green solvents in membrane fabrication.

differences below 2 $MPa^{1/2}$ as suitable for dissolution. Sanchez-Lengeling *et al.* developed a Bayesian machine learning model based on Gaussian processes to predict HSPs for 193 solvents and 31 polymers using molecular access system (MACCS) keys and Morgan fingerprints as molecular descriptors. The model achieved prediction accuracies with R^2 values ranging from 0.56 to 0.83.[232] Moreover, Kern *et al.* trained random forests and multilayer perceptron neural networks on a dataset of 3373 polymers and 51 solvents, predicting room-temperature polymer–solvent solubility.[233] Their polymer representations combined three hierarchical levels of descriptors (*e.g.*, atomic triplets, chemical building blocks, and QSPR descriptors), while solvent representations used one-hot encoding or structural fingerprints, enabling accurate classification of polymer solubility in diverse solvents.

One of the primary limitations in applying AI to green solvent design and membrane development is data sparsity, particularly for novel solvents such as Cyrene™, NADESs, and DESs.[234,235] Unlike conventional solvents such as NMP or DMF, which benefit from abundant experimental datasets, these greener alternatives often lack comprehensive, high-quality data covering key parameters such as polymer solubility, membrane morphology, toxicity, and environmental impact. This scarcity restricts the performance and generalizability of conventional data-driven models. To overcome this limitation, advanced AI approaches have incorporated techniques such as transfer learning, which leverages knowledge from well-characterized systems to make predictions in less-explored domains and data augmentation, where synthetic or simulated data are generated from molecular descriptors. Physics-informed machine learning, which integrates solubility theories or thermodynamic constraints into model architectures, is also gaining traction. Additionally, semi-supervised learning can exploit both labelled and unlabelled data to improve prediction accuracy. While these methods show considerable promise, the long-term success of AI in green solvent discovery will ultimately depend on improving data availability through systematic experimental reporting and the development of open-access databases.

Fig. 17 illustrates a general overview of the data-driven algorithm execution process.[236] A typical data-driven model workflow comprises three essential components, namely data, representation, and model, which operate in two main phases: training and prediction. In the training phase, raw input data undergo pre-processing steps such as duplicate removal, normalization, dimensionality reduction, transformation, and feature data extraction and selection. The refined data are then used in the learning stage to develop a trained model, followed by error analysis to assess and optimize the performance. This structured approach enables the development of accurate, efficient, and real-time prediction models, with the quality and relevance of the input data being critical for generating reliable outputs.

To conclude this section, the various AI models discussed are summarized as a workflow in Fig. 18 for predicting green solvent–polymer compatibility in membrane fabrication. In general, an AI workflow begins with data input for model training. The trained AI model then generates the desired output through a structured learning process. Finally, the output is validated against experimental or benchmark data to ensure the reliability and accuracy of the AI model.[237]

11. Conclusion

The transition to green solvents in membrane technology represents a pivotal stride toward sustainable separation processes, addressing the environmental and health concerns associated with traditional solvents such as NMP and DMF. This review has critically assessed the applications, advantages, and limitations of seven major classes of green solvents, namely, esters, polar aprotic, dipolar aprotic, polar protic, non-

polar aprotic, organic salts, and oils in both gas and liquid separation. While these alternatives demonstrate substantial promise, their industrial implementation faces practical and economic challenges. The following are the concluding remarks.

1. Esters such as GBL and TEP offer excellent polymer solubility and tunable properties for membrane fabrication. GBL has shown success in CO_2-selective membranes, whereas TEP is a greener alternative for PVDF membrane synthesis. However, their scalability is constrained by high production costs and energy-intensive synthesis (*e.g.*, GBL requires high-pressure conditions). Additionally, the lower solvent power in TEP compared to NMP may result in suboptimal membrane morphology, necessitating formulation optimization.

2. Among polar aprotic solvents, biomass-derived Cyrene™ stands out due to its low toxicity and strong solvating power, proving effective in polyimide and polysulfone membranes while mitigating macrovoid formation. However, its reliance on the hydrogenation of levoglucosenone may limit its availability. Similarly, while 2-MeTHF is biodegradable, its high volatility complicates the phase inversion processes. GVL holds promise for nanofiltration membranes but demands further functionalization to improve CO_2 capture due to its low polarity restricting interactions with acidic gases.

3. Dipolar aprotic solvents such as DMSO are valued for their broad polymer compatibility and low toxicity, supporting their use in ultrafiltration and gas separation. However, the high boiling point of DMSO complicates solvent recovery. Alternatives like Tamisolve® NxG and Polarclean are excellent NMP replacements, but their high viscosity can lead to uneven pore formation during membrane fabrication.

4. Polar protic solvents, such as Agnique® AMD 3L, have demonstrated their potential in PES hollow fiber membranes, but solvent retention remains an issue, particularly in biomedical applications.

5. ILs and DESs provide highly customizable platforms, with ILs exhibiting strong chemisorption for CO_2 capture. However, ILs face limitations including high synthesis costs, toxicity concerns, and recycling difficulties. DESs are more cost-effective and biodegradable but suffer from viscosity and thermal stability issues that hinder membrane processing. Emerging research into NADESs is promising, although industrial validation is still needed.

6. Biodegradable oils such as palm oil, RBO, and sunflower oil show potential in ELM applications for the extraction of heavy metals and organic pollutants. Palm oil and RBO enhance emulsion stability but exhibit high viscosities that slow mass transfer. Sunflower oil offers superior reusability (*e.g.*, up to 4 cycles) but faces challenges in demulsification efficiency. The variable composition of these oils, dependent on source and harvest conditions, can lead to inconsistent separation performances.

7. A general solvent selection workflow that incorporates sustainability and solvent recovery considerations is proposed. First, evaluate solvent sustainability using established guides such as CHEM21, GSK solvent guide, and REACH classifications, and eliminate solvents with high toxicity or regulatory concerns. Next, perform polymer–solvent compatibility screening by calculating HSP and RED, selecting solvents with RED < 1. This is followed by solubility tests to assess the homogeneity and viscosity of dope solutions. Membrane fabrication and performance testing are then conducted. Finally, evaluate solvent recovery and carry out a comprehensive life cycle assessment (LCA) alongside an economic feasibility study.

12. Challenges and future prospects

Although various alternative green solvents have been proposed for gas and liquid separation, there is an urgent need to continue advancing the development of more industrially feasible solvents for real-world applications. Accordingly, the following challenges and perspectives are outlined to guide future efforts toward sustainable green solvent development and implementation.

1. Polymeric membranes are typically fabricated using solution-based methods such as NIPS or TIPS. These techniques are highly reliant on solvents for polymer dissolution, which significantly influences the resulting membrane. One of the key challenges in employing green solvents is the validation of solvent–polymer compatibility through HSP evaluation. Although green solvent membranes offer clear environmental benefits, concerns remain regarding the sustainability of green solvent production. Upstream emissions and high energy consumption during synthesis can offset their ecological benefits.[238] This is particularly relevant for ILs and DESs, which often require elevated temperatures due to their inherent high viscosity, low conductivity, and limited diffusion, resulting in substantial energy usage.[239]

2. A broader range of green solvents that are characterized by low toxicity, biodegradability, and favorable solvation properties should be explored beyond those currently in use. Additional research into their compatibility with various polymer systems and processing techniques is essential to unlock their full potential for scalable membrane production.

3. Scalability remains a critical bottleneck when transitioning green solvent-based membranes from the laboratory to industrial applications. For commercialization, membranes must deliver a high separation performance, cost-effectiveness, desired separation performance, and long-term operational stability. SLMs limit mechanical stability due to pressure fluctuations, further impeding their large-scale application.

4. Economic viability is also a major consideration. ILs are generally more expensive than DESs, though some ILs can be synthesized *via* cost-effective acid–base reactions such as [MTBDH][TFE], [MTBDH][Im], [MTBDH][PhO], [MTBDH][TFPA], and [MTBDH][Pyrr], which minimize wastewater production and improve sustainability.[239,240]

5. In contrast, DESs are characterized by lower cost, scalability, and chemical inertness to water, making them easier to handle and store.[241,242] They offer promising potential for CO_2 capture applications due to their affordability and tunability. However, current research is insufficient to fully optimize DES

structures for enhanced CO_2 adsorption performance. Future work should focus on tailoring DES compositions to improve CO_2 capture capabilities, paving the way for broader industrial adoption.[241]

6. To accelerate green solvent selection and membrane development, advanced artificial intelligence (AI) tools can be leveraged. These tools facilitate high-throughput screening of solvent candidates, reducing reliance on trial-and-error experimentation. Furthermore, AI can aid in guiding solvent design by identifying molecular modifications that enhance polymer dissolution while preserving eco-friendly characteristics. Additionally, cross-disciplinary collaboration between chemical engineers and computational scientists is crucial to accelerate the development of high-performance green solvent membranes.

7. The compatibility of green solvents with polymers directly influences membrane performance, lifespan, and fabrication costs. To fully assess their environmental and economic impacts, life cycle assessment (LCA) and techno-economic analysis (TEA) should be incorporated. Achieving membranes that combine excellent performance, low cost, scalability, and sustainability remains a significant challenge. Nevertheless, continued progress in green solvent research is essential to advance carbon reduction efforts and enhance the sustainability of membrane-based separation technologies.

8. The adoption of green solvents in membrane technology signifies not only an environmental necessity but also a technological advancement. While several barriers ranging from cost and scalability to physicochemical limitations remain, steady progress in developing bio-based, low toxicity alternatives signals a clear pathway toward sustainable separation processes. Strategic collaboration between industry, academia, and regulatory bodies combined with policy incentives and continued innovation will be crucial for transforming laboratory-scale successes into practical, industrial-scale applications, thereby aligning membrane technology with global sustainable development goals (SDGs).

Author contributions

Boon Kee Voon and Yen Juin Yap: writing – original draft, writing – review & editing, visualization. Wai Fen Yong: writing – review & editing, supervision, project administration, funding acquisition.

Conflicts of interest

There are no conflicts to declare.

Data availability

No primary research results, software or code have been included and no new data were generated or analysed as part of this review.

Acknowledgements

The authors would like to acknowledge financial support provided by the National Natural Science Foundation of China (grant number: 22108118), the State Key Laboratory of Physical Chemistry of Solid Surfaces, Xiamen University (grant number: 2024X32), the Xiamen University Malaysia Research Fund (grant number: XMUMRF/2024-C14/IENG/0073 and ICOE/0003), and Hengyuan International Sdn. Bhd. (grant number: EENG/0003).

References

1 P. P. Groumpos, *IFAC Pap. OnLine*, 2021, **54**, 464–471.
2 M. Klemke-Pitek and M. Majchrzak, *Energies*, 2022, **15**, 2192.
3 I. Siedschlag and W. Yan, *J. Cleaner Prod.*, 2021, **310**, 127554.
4 T. C. Merkel, H. Lin, X. Wei and R. Baker, *J. Membr. Sci.*, 2010, **359**, 126–139.
5 D. S. Sholl and R. P. Lively, *Nature*, 2016, **532**, 435–437.
6 T. A. Saleh and V. K. Gupta, in *Nanomaterial and Polymer Membranes*, ed. T. A. Saleh and V. K. Gupta, Elsevier, 2016, pp. 1–23.
7 E. Lasseuguette and B. Comesaña-Gándara, *Membranes*, 2022, **12**, 207.
8 R. Hou, C. Fong, B. D. Freeman, M. R. Hill and Z. Xie, *Sep. Purif. Technol.*, 2022, **300**, 121863.
9 J. Y. Teh and W. F. Yong, *Carbon Capture Sci. Technol.*, 2024, **13**, 100334.
10 W. S. W. Ong and W. F. Yong, *Prog. Mater. Sci.*, 2025, **152**, 101454.
11 F. Pena-Pereira and M. Tobiszewski, in *The Application of Green Solvents in Separation Processes*, ed. F. Pena-Pereira and M. Tobiszewski, Elsevier, 2017, pp. 3–16.
12 B. Metz, O. Davidson, H. De Coninck, M. Loos and L. Meyer, *IPCC Special Report on Carbon Dioxide Capture and Storage*, Cambridge University Press, Cambridge, 2005.
13 H. H. Wang, J. T. Jung, J. F. Kim, S. Kim, E. Drioli and Y. M. Lee, *J. Membr. Sci.*, 2019, **574**, 44–54.
14 J. Sherwood, F. Albericio and B. G. de la Torre, *ChemSusChem*, 2024, **17**, 202301639.
15 C. M. Alder, J. D. Hayler, R. K. Henderson, A. M. Redman, L. Shukla, L. E. Shuster and H. F. Sneddon, *Green Chem.*, 2016, **18**, 3879–3890.
16 R. K. Henderson, C. Jiménez-González, D. J. C. Constable, S. R. Alston, G. G. A. Inglis, G. Fisher, J. Sherwood, S. P. Binks and A. D. Curzons, *Green Chem.*, 2011, **13**, 854–862.
17 D. Prat, A. Wells, J. Hayler, H. Sneddon, C. R. McElroy, S. Abou-Shehada and P. J. Dunn, *Green Chem.*, 2016, **18**, 288–296.
18 S. U. Hong, Y. Wang, L. S. Soh and W. F. Yong, *Green Chem.*, 2023, **25**, 4501–4512.

19 B. Nanda, M. Sailaja, P. Mohapatra, R. K. Pradhan and B. B. Nanda, *Mater. Today: Proc.*, 2021, **47**, 1234–1240.
20 A. Figoli, T. Marino, S. Simone, E. Di Nicolò, X. M. Li, T. He, S. Tornaghi and E. Drioli, *Green Chem.*, 2014, **16**, 4034–4059.
21 M. A. Rasool and I. F. J. Vankelecom, *Green Chem.*, 2019, **21**, 1054–1064.
22 T. Marino, F. Galiano, A. Molino and A. Figoli, *J. Membr. Sci.*, 2019, **580**, 224–234.
23 L. S. Soh, S. U. Hong, C. Z. Liang and W. F. Yong, *Chem. Eng. J.*, 2023, **478**, 147451.
24 A. Banger, A. Srivastava, A. Yadav, R. Sharma and M. Srivastava, *Green Chem. Technol. Lett.*, 2023, **9**, 01–14.
25 D. Zou, S. P. Nunes, I. F. J. Vankelecom, A. Figoli and Y. M. Lee, *Green Chem.*, 2021, **23**, 9815–9843.
26 S. A. Naziri Mehrabani, V. Vatanpour and I. Koyuncu, *Sep. Purif. Technol.*, 2022, **298**, 121691.
27 C. M. Hansen, *Hansen Solubility Parameters: A User's Handbook, Second Edition*, CRC Press, 2007.
28 S. Venkatram, C. Kim, A. Chandrasekaran and R. Ramprasad, *J. Chem. Inf. Model.*, 2019, **59**, 4188–4194.
29 C. M. Hansen, *Prog. Org. Coat.*, 2004, **51**, 109–112.
30 M. A. Rasool, P. P. Pescarmona and I. F. J. Vankelecom, *ACS Sustainable Chem. Eng.*, 2019, **7**, 13774–13785.
31 T. Marino, E. Blasi, S. Tornaghi, E. Di Nicolò and A. Figoli, *J. Membr. Sci.*, 2018, **549**, 192–204.
32 R. Kanawade, A. Kumar, D. Pawar, K. Vairagi, D. Late, S. Sarkar, R. K. Sinha and S. Mondal, *Opt. Express*, 2019, **27**, 7277–7290.
33 M. M. Crowley, A. Fredersdorf, B. Schroeder, S. Kucera, S. Prodduturi, M. A. Repka and J. W. McGinity, *Eur. J. Pharm. Sci.*, 2004, **22**, 409–418.
34 A. Benazzouz, L. Moity, C. Pierlot, M. Sergent, V. Molinier and J.-M. Aubry, *Ind. Eng. Chem. Res.*, 2013, **52**, 16585–16597.
35 O. Gronwald and M. Weber, *J. Appl. Polym. Sci.*, 2019, **137**, 48419.
36 F. Russo, F. Galiano, F. Pedace, F. Aricò and A. Figoli, *ACS Sustainable Chem. Eng.*, 2020, **8**, 659–668.
37 J. D. Vincent, K. Srinivas and J. W. King, *J. Am. Oil Chem. Soc.*, 2012, **89**, 1585–1597.
38 X. Jiang, W. F. Yong, J. Gao, D.-D. Shao and S.-P. Sun, *J. Membr. Sci.*, 2021, **635**, 119530.
39 W. Xie, A. Tiraferri, B. Liu, P. Tang, F. Wang, S. Chen, A. Figoli and L.-Y. Chu, *ACS Sustainable Chem. Eng.*, 2020, **8**, 91–101.
40 T. Marino, F. Russo and A. Figoli, *Membranes*, 2018, **8**, 71.
41 M. Díaz de los Ríos and E. Hernández Ramos, *SN Appl. Sci.*, 2020, **2**, 676.
42 F. Cakar, D. Sakar, O. Cankurtaran and F. Karaman, *Eur. Polym. J.*, 2007, **43**, 507–513.
43 E. G. Al-Sakkari, A. Ragab, M. Amer, O. Ajao, M. Benali, D. C. Boffito, H. Dagdougui and M. Amazouz, *Digit. Chem. Eng.*, 2025, **14**, 100207.
44 C. Li, Z. Li, X. Liu, J. Xu and C. Zhang, *J. Mol. Liq.*, 2024, **408**, 125319.
45 J. Pavliš, A. Mathers, M. Fulem and M. Klajmon, *Mol. Pharm.*, 2023, **20**, 3960–3974.
46 J. Huang, H. Tang, X. Huang, Z. Feng, P. Su and W. Li, *J. Membr. Sci.*, 2023, **668**, 121238.
47 H. Wu, Z. Xie, G. Li, L. Zheng, Z. Zhao, J. He, Y. Shen, J. Hu, Z. Peng, G. Zhong, L. Xing and W. Li, *J. Energy Chem.*, 2024, **93**, 193–201.
48 D. W. Hwang, P. Kashinathan, J. M. Lee, J. H. Lee, U. h. Lee, J.-S. Hwang, Y. K. Hwang and J.-S. Chang, *Green Chem.*, 2011, **13**, 1672–1675.
49 Sigma-Aldrich, Safety data sheet for γ-butyrolactone, **https://www.sigmaaldrich.com/SG/en/sds/aldrich/b103608?userType=anonymous**, (accessed 18 June 2025).
50 Merck, Safety data sheet for glycerol triacetate, **https://www.merckmillipore.com/SG/en/product/msds/MDA_CHEM-108238?ReferrerURL=https%3A%2F%2Fwww.google.com%2F**, (accessed 18 June 2025).
51 Sigma-Aldrich, Safety data sheet for triethyl phosphate, **https://www.sigmaaldrich.com/SG/en/sds/aldrich/538728?userType=undefined**, (accessed 18 June 2025).
52 Sigma-Aldrich, Safety data sheet for 2-methyltetrahydrofuran, **https://www.sigmaaldrich.com/SG/en/sds/sial/673277?userType=anonymous**, (accessed 18 June 2025).
53 Sigma-Aldrich, Safety data sheet for γ-valerolactone, **https://www.sigmaaldrich.com/SG/en/sds/aldrich/v403?userType=anonymous**, (accessed 18 June 2025).
54 Merck, Safety data sheet for dimethyl sulfoxide (DMSO), **https://www.merckmillipore.com/SG/en/product/msds/MM_NF-20-139?ReferrerURL=https%3A%2F%2Fwww.google.com%2F**, (accessed 18 June 2025).
55 Eastman, Safety data sheet for TamiSolve NxG, **https://www.eastman.com/en/products/product-detail/71103844/eastman-tamisolve-nxg**, (accessed 18 June 2025).
56 A. Kumar, A. Sharma, B. G. de la Torre and F. Albericio, *Green Chem. Lett. Rev.*, 2021, **14**, 545–550.
57 Sigma-Aldrich, Safety data sheet for *N*,*N*-dimethylacetamide, **https://www.sigmaaldrich.com/SG/en/product/aldrich/185884**, (accessed 1 January, 2025).
58 Sigma-Aldrich, Safety data sheet for Cyrene, **https://www.sigmaaldrich.com/SG/en/sds/sial/807796?userType=anonymous**, (accessed 18 June 2025).
59 C. Roth, Safety data sheet for *N*,*N*-dimethyl lactamid, **https://www.carlroth.com/com/en/alternative-solvents/nn-dimethyl-lactamid/p/22l0.1**, (accessed 18 June 2025).
60 Chemos, Safety data sheet for palm oil, **https://www.chemos.de/import/data/msds/GB_en/8002-75-3-A0050032-GB-en.pdf**, (accessed 18 June 2025).
61 N. O. Oils, Safety data sheet for rice bran oil, **https://www.nhrorganicoils.com/uploads/20180305135645e_Rice_Bran_SDS.pdf**, (accessed 18 June 2025).
62 N. O. Oils, Safety data sheet for sunflower oil, **https://www.nhrorganicoils.com/uploads/20171214142435e_Sunflower_SDS.pdf**, (accessed 18 June 2025).
63 National Center for Biotechnology Information (NCBI), **https://pubmed.ncbi.nlm.nih.gov/**, (accessed 8 August 2025).

64 N. Li, X. Han, H. Lv, Y. Jin and J. Yu, *J. Cleaner Prod.*, 2025, **486**, 144452.
65 N. Ismail, Q. Zhou, Q. Wang, Z. Cui, N. Skoglund and N. Tavajohi, *Green Chem.*, 2023, **25**, 7259–7272.
66 ChemAnalyst, Dimethylformamide Market Analysis: Industry Market Size, Plant Capacity, Production, Operating Efficiency, Demand & Supply, End-User Industries, Sales Channel, Regional Demand, Company Share, Manufacturing Process, 2015–2032, **https://www.chemanalyst.com/industry-report/dimethylformamide-market-2876**, (accessed 8 August 2025).
67 J. Ma, L. Hu, J. Yao, Z. Wang, A. Li, D. Hrynsphan, T. Savitskaya and J. Chen, *J. Environ. Chem. Eng.*, 2024, **12**, 112038.
68 F. Marclay, D. Pazos, O. Delémont, P. Esseiva and C. Saudan, *Forensic Sci. Int.*, 2010, **198**, 46–52.
69 M. J. Quinn and D. Ziolkowski, in *Wildlife Toxicity Assessments for Chemicals of Military Concern*, ed. M. A. Williams, G. Reddy, M. J. Quinn and M. S. Johnson, Elsevier, 2015, pp. 291–301, DOI: **10.1016/B978-0-12-800020-5.00017-X**.
70 OECD, Triethylphosphate, **https://hpvchemicals.oecd.org/ui/SIDS_Details.aspx?id=bface0ce-8c3a-4057-a85b-4abd61f7b17a**, (accessed 8 August 2025).
71 S. Gundekari and S. K. Karmee, *Molecules*, 2024, **29**, 242.
72 CarlRoth, **https://www.carlroth.com/com/en/**, (accessed 8 August 2025).
73 T. Brouwer and B. Schuur, *ACS Sustainable Chem. Eng.*, 2020, **8**, 14807–14817.
74 R. P. B. Ashok, P. Oinas and S. Forssell, *Renewable Energy*, 2022, **190**, 396–407.
75 SigmaAldrich, **https://www.carlroth.com/com/en/**, (accessed 8 August 2025).
76 A. J. Greer, J. Jacquemin and C. Hardacre, *Molecules*, 2020, **25**, 5207.
77 H. Passos, M. G. Freire and J. A. P. Coutinho, *Green Chem.*, 2014, **16**, 4786–4815.
78 Virtue, Deep Eutectic Solvent Market Research Report, **https://virtuemarketresearch.com/report/deep-eutectic-solvent-market**, (accessed 8 August 2025).
79 D. J. Murphy, K. Goggin and R. R. M. Paterson, *CABI Agric. Biosci.*, 2021, **2**, 39.
80 Y. Purbawa, I. G. M. Y. Bakti, H. J. Purba, N. J. Astrini, R. P. Putra and S. Sumaedi, *J. Revenue Pricing Manag.*, 2023, **22**, 446–454.
81 J. S. Godber, in *Gourmet and Health-Promoting Specialty Oils*, ed. R. A. Moreau and A. Kamal-Eldin, AOCS Press, 2009, pp. 377–408, DOI: **10.1016/B978-1-893997-97-4.50020-6**.
82 M. Kabir, U. Umara, M. M. Alam and C. K. Saha, *J. Agric. Mach. Bioresour. Eng.*, 2016, **7**, 33–40.
83 A. Kabutey, D. Herák and Č. Mizera, *Foods*, 2022, **11**, 2866.
84 Oilseeds: World Markets and Trade, **https://www.fas.usda.gov/data/oilseeds-world-markets-and-trade-07112025**, (accessed 8 August 2025).
85 G. V. Theodorakopoulos, D. S. Karousos, K. G. Mansouris, A. A. Sapalidis, E. P. Kouvelos and E. P. Favvas, *Int. J. Greenhouse Gas Control*, 2022, **114**, 103588.
86 Y. Dai, X. Ruan, F. Bai, M. Yu, H. Li, Z. Zhao and G. He, *Appl. Surf. Sci.*, 2016, **360**, 164–173.
87 C. V. Lacerda, M. J. Carvalho, A. R. Ratton, I. P. Soares and L. E. Borges, *J. Braz. Chem. Soc.*, 2015, **26**, 1625–1631.
88 L. N. Silva, V. L. Gonçalves and C. J. Mota, *Catal. Commun.*, 2010, **11**, 1036–1039.
89 M. Z. Fiume, *Int. J. Toxicol.*, 2003, **22**, 1–10.
90 R. G. Penido, R. B. Costa, F. G. Delolo, E. V. Gusevskaya and E. N. dos Santos, *ACS Sustainable Chem. Eng.*, 2025, **13**, 5828–5837.
91 G. V. Theodorakopoulos, D. S. Karousos, C. M. Veziri, E. P. Kouvelos, A. A. Sapalidis and E. P. Favvas, *J. Membr. Sci. Lett.*, 2023, **3**, 100057.
92 E. K. Chatzidaki, E. P. Favvas, S. K. Papageorgiou, N. K. Kanellopoulos and N. V. Theophilou, *Eur. Polym. J.*, 2007, **43**, 5010–5016.
93 S.-H. Choi, A. Brunetti, E. Drioli and G. Barbieri, *Sep. Sci. Technol.*, 2010, **46**, 1–13.
94 E. P. Favvas, S. K. Papageorgiou, J. W. Nolan, K. L. Stefanopoulos and A. C. Mitropoulos, *J. Appl. Polym. Sci.*, 2013, **130**, 4490–4499.
95 L. Sheng, J. Ren, K. Hua, H. Li, Y. Feng and M. Deng, *J. Membr. Sci.*, 2020, **595**, 117580.
96 Y. Alqaheem and A. A. Alomair, *ACS Omega*, 2020, **5**, 6330–6335.
97 D. Zhao, J. Ren, Y. Wang, Y. Qiu, H. Li, K. Hua, X. Li, J. Ji and M. Deng, *J. Membr. Sci.*, 2017, **521**, 104–113.
98 N. Soltani and O. Bakhtiari, *Korean J. Chem. Eng.*, 2021, **38**, 1469–1486.
99 M. A. Rasool and I. F. J. Vankelecom, *J. Membr. Sci.*, 2021, **618**, 118674.
100 H.-H. Chang, C.-H. Tsai, H.-C. Wei and L.-P. Cheng, *Membr. Water Treat.*, 2014, **5**, 41–56.
101 K. P. Nandhini, N. Cele, B. G. de la Torre and F. Albericio, *Green Chem. Lett. Rev.*, 2024, **17**, 2330639.
102 H.-R. Yang, Y.-H. Huang, C.-F. Wang and T.-S. Chung, *Desalination*, 2023, **566**, 116934.
103 C. Chen, V. Reddy Tatagari, H. Lin and L. Shaw, *J. Energy Chem.*, 2023, **78**, 240–245.
104 J. Chang, J. Zuo, L. Zhang, G. S. O'Brien and T.-S. Chung, *J. Membr. Sci.*, 2017, **539**, 295–304.
105 S. Fadhil, T. Marino, H. F. Makki, Q. F. Alsalhy, S. Blefari, F. Macedonio, E. D. Nicolò, L. Giorno, E. Drioli and A. Figoli, *Chem. Eng. Process.*, 2016, **102**, 16–26.
106 C. P. Jiménez-Gómez, C. García-Sancho, J. A. Cecilia and P. Maireles-Torres, in *Green Sustainable Process for Chemical and Environmental Engineering and Science*, ed. I. R. Boddula and A. M. Asiri, Elsevier, 2021, pp. 75–98.
107 H. H. Khoo, L. L. Wong, J. Tan, V. Isoni and P. Sharratt, *Resour., Conserv. Recycl.*, 2015, **95**, 174–182.
108 A. M. Shenoy, R. Thür, B. van Duffel and I. F. J. Vankelecom, *J. Membr. Sci.*, 2025, **717**, 123573.

109 I. T. Horváth, H. Mehdi, V. Fábos, L. Boda and L. T. Mika, *Green Chem.*, 2008, **10**, 238–242.
110 S. Dutta, K. Iris, D. C. Tsang, Y. H. Ng, Y. S. Ok, J. Sherwood and J. H. Clark, *Chem. Eng. J.*, 2019, **372**, 992–1006.
111 D. M. Alonso, S. G. Wettstein and J. A. Dumesic, *Green Chem.*, 2013, **15**, 584–595.
112 F. Kerkel, M. Markiewicz, S. Stolte, E. Müller and W. Kunz, *Green Chem.*, 2021, **23**, 2962–2976.
113 F. Boissou, S. Baranton, M. Tarighi, K. De Oliveira Vigier and C. Coutanceau, *J. Electroanal. Chem.*, 2019, **848**, 113257.
114 D. Deng, G. Han, Y. Jiang and N. Ai, *J. Chem. Eng. Data*, 2015, **60**, 104–111.
115 H. Q. Lê, J.-P. Pokki, M. Borrega, P. Uusi-Kyyny, V. Alopaeus and H. Sixta, *Ind. Eng. Chem. Res.*, 2018, **57**, 15147–15158.
116 S. Santoro, J. Occhiuzzi, M. Aquino, A. Politano, S. Straface, G. D'Andrea, C. Carrillo, R. Mallada, A. Garcia, H. Estay, D. Xevgenos, P. Argurio and E. Curcio, *Sep. Purif. Technol.*, 2024, **342**, 127042.
117 R. Shimizu and H. Tanaka, *Nat. Commun.*, 2015, **6**, 7407.
118 F. Wang, J. Zhao and L. Hu, *Int. J. Netw. Virtual Organ.*, 2018, **20**, 14–34.
119 V. Altun, J.-C. Remigy and I. F. J. Vankelecom, *J. Membr. Sci.*, 2017, **524**, 729–737.
120 M. H. D. A. Farahani and T.-S. Chung, *Sep. Purif. Technol.*, 2019, **209**, 182–192.
121 M. A. Rasool and I. F. J. Vankelecom, *Membranes*, 2021, **11**, 418.
122 R. D. Nyamiati, Y. Rahmawati, A. Altway and S. Nurkhamidah, *IOP Conf. Ser.: Mater. Sci. Eng.*, 2021, **1143**, 012063.
123 S. Laurichesse and L. Avérous, *Prog. Polym. Sci.*, 2014, **39**, 1266–1290.
124 K. M. Fung, C. L. Heald, J. H. Kroll, S. Wang, D. S. Jo, A. Gettelman, Z. Lu, X. Liu, R. A. Zaveri, E. C. Apel, D. R. Blake, J. L. Jimenez, P. Campuzano-Jost, P. R. Veres, T. S. Bates, J. E. Shilling and M. Zawadowicz, *Atmos. Chem. Phys.*, 2022, **22**, 1549–1573.
125 P. E. Correa and D. P. Riley, *J. Org. Chem.*, 1985, **50**, 1787–1788.
126 N.-G. Park, *Nat. Sustain.*, 2021, **4**, 192–193.
127 W. A. Willford, *Toxicity of Dimethyl Sulfoxide (DMSO) to Fish*, 1967.
128 R. Vignes, Dimethyl sulfoxide (DMSO) - A "new" clean, unique, superior solvent, American Chemical Society Annual Meeting, 2000.
129 S. Yousef, M. Tatariants, M. Tichonovas, Z. Sarwar, I. Jonuškienė and L. Kliucininkas, *Resour., Conserv. Recycl.*, 2019, **145**, 359–369.
130 E. E. Vogin, S. Carson, G. Cannon, C. R. Linegar and L. F. Rubin, *Toxicol. Appl. Pharmacol.*, 1970, **16**, 606–612.
131 F. E. Ala'a, F. Alsoubani, K. I. Assaf, W. M. Nau, C. Troll and A. K. Qaroush, *RSC Adv.*, 2016, **6**, 22090–22093.
132 F. E. Ala'a, A. K. Qaroush, F. Alsoubani, T. M. Pehl, C. Troll, B. Rieger, B. A. Al-Maythalony and K. I. Assaf, *RSC Adv.*, 2018, **8**, 37757–37764.
133 G. Latini, M. Signorile, F. Rosso, A. Fin, M. d'Amora, S. Giordani, F. Pirri, V. Crocella, S. Bordiga and S. Bocchini, *J. CO_2 Util.*, 2022, **55**, 101815.
134 Substance Infocard of 1-butylpyrrolidin-2-one, **https://echa.europa.eu/substance-information/-/substanceinfo/100.020.399**).
135 J. Sherwood, H. L. Parker, K. Moonen, T. J. Farmer and A. J. Hunt, *Green Chem.*, 2016, **18**, 3990–3996.
136 A. Kumar, M. Alhassan, J. Lopez, F. Albericio and B. G. de la Torre, *ChemSusChem*, 2020, **13**, 5288–5294.
137 A. Randová, L. Bartovská, P. Morávek, P. Matějka, M. Novotná, S. Matějková, E. Drioli, A. Figoli, M. Lanč and K. Friess, *J. Mol. Liq.*, 2016, **224**, 1163–1171.
138 A. Kumar, A. Sharma, B. G. de la Torre and F. Albericio, *Green Chem. Lett. Rev.*, 2021, **14**, 545–550.
139 P. Ortiz-Albo, V. D. Alves, I. Kumakiri, J. Crespo and L. A. Neves, *J. Membr. Sci.*, 2024, **693**, 122346.
140 D. V. Bhalani, B. Nutan and A. K. S. Chandel, in *Encyclopedia of Green Materials*, ed. C. Baskar, S. Ramakrishna and A. D. La Rosa, Springer Nature Singapore, Singapore, 2022, pp. 1–9, DOI: **10.1007/978-981-16-4921-9_223-1**.
141 F. Russo, C. Ursino, B. Sayinli, I. Koyuncu, F. Galiano and A. Figoli, *Clean Technol.*, 2021, **3**, 761–786.
142 N. T. Hassankiadeh, Z. Cui, J. H. Kim, D. W. Shin, S. Y. Lee, A. Sanguineti, V. Arcella, Y. M. Lee and E. Drioli, *J. Membr. Sci.*, 2015, **479**, 204–212.
143 L. Cseri and G. Szekely, *Green Chem.*, 2019, **21**, 4178–4188.
144 P. Ray, T. Hughes, C. Smith, M. Hibbert, K. Saito and G. P. Simon, *Polym. Chem.*, 2019, **10**, 3334–3341.
145 K. O. Novisi, C. M. Leah and C. E. M. Banothile, in *Solvents, Ionic Liquids and Solvent Effects*, ed. G.-M. Daniel and M. Magdalena, IntechOpen, Rijeka, 2019, ch. 1, DOI: **10.5772/intechopen.86502**.
146 S. Kudo, X. Huang, S. Asano and J.-i. Hayashi, *Energy Fuels*, 2021, **35**, 9809–9824.
147 A. T. Bridge, N. P. Wamble, M. S. Santoso, J. F. Brennecke and B. D. Freeman, *J. Membr. Sci.*, 2024, **691**, 122221.
148 A. T. Bridge, B. J. Pedretti, J. F. Brennecke and B. D. Freeman, *J. Membr. Sci.*, 2022, **644**, 120173.
149 P. Tomietto, F. Russo, F. Galiano, P. Loulergue, S. Salerno, L. Paugam, J.-L. Audic, L. De Bartolo and A. Figoli, *J. Membr. Sci.*, 2022, **643**, 120061.
150 Y. Wibisono, V. Noviani, A. T. Ramadhani, L. A. Devianto and A. A. Sulianto, *Results Eng.*, 2022, **16**, 100712.
151 D. Kong and A. V. Dolzhenko, *Sustainable Chem. Pharm.*, 2022, **25**, 100591.
152 N. Stini, P. Gkizis and C. Kokotos, *Green Chem.*, 2022, **24**, 6435–6449.
153 L. Lebanov, P. K. Chadalawada, D. M. Dissanayaka, S. Alwis, D. Heier, D. E. Richardson and B. Paull, *Green Anal. Chem.*, 2025, **13**, 100240.

154 Q. Liu, J. Liu, M. Li, T. Yu, M. Hu, P. Jia, N. Qi and Z. Chen, *Colloids Surf., A*, 2022, **654**, 130108.
155 P. Dżygiel and P. P. Wieczorek, in *Liquid Membranes*, ed. V. S. Kislik, Elsevier, Amsterdam, 2010, pp. 73–140.
156 M. Zia ul Mustafa, H. bin Mukhtar, N. A. H. Md Nordin, H. A. Mannan, R. Nasir and N. Fazil, *Chem. Eng. Technol.*, 2019, **42**, 2580–2593.
157 C. Yang, J. Cavalcante, B. B. de Freitas, K. J. Lauersen and G. Szekely, *Chem. Eng. J.*, 2023, **470**, 144153.
158 G. M. Shi, M. H. D. A. Farahani, J. Y. Liu and T.-S. Chung, *J. Membr. Sci.*, 2019, **588**, 117202.
159 T. Marino, F. Galiano, S. Simone and A. Figoli, *Environ. Sci. Pollut. Res.*, 2019, **26**, 14774–14785.
160 Y. X. Foong, L. H. Yew and P. V. Chai, *Mater. Today: Proc.*, 2021, **46**, 2092–2097.
161 Y. F. Ong, Y. T. Wong and P. V. Chai, *Mater. Today: Proc.*, 2022, **64**, 1655–1660.
162 N. Alqadhi, M. H. Abdellah, S. Nematulloev, O. F. Mohammed, M. A. Abdulhamid and G. Szekely, *Sep. Purif. Technol.*, 2024, **328**, 125072.
163 C. Ursino, F. Russo, R. M. Ferrari, M. P. De Santo, E. Di Nicolò, T. He, F. Galiano and A. Figoli, *J. Membr. Sci.*, 2020, **608**, 118216.
164 D. Zou, S. M. Jeon, H. W. Kim, J. Y. Bae and Y. M. Lee, *J. Membr. Sci.*, 2021, **637**, 119632.
165 D. Zou, H. W. Kim, S. M. Jeon and Y. M. Lee, *J. Membr. Sci.*, 2022, **644**, 120101.
166 R. Hardian, R. M. Cywar, E. Y. X. Chen and G. Szekely, *J. Membr. Sci. Lett.*, 2022, **2**, 100016.
167 J. Zhu, X. Wang, Q. Jiang, J. Duan and H. Wang, *J. Colloid Interface Sci.*, 2024, **667**, 32–43.
168 T. Götz, B. Achenbach and T. Schiestel, *ACS Appl. Polym. Mater.*, 2023, **5**, 4411–4418.
169 S. Uebele, K. Johann, T. Goetz, O. Gronwald, M. Ulbricht and T. Schiestel, *J. Appl. Polym. Sci.*, 2021, **138**, 50935.
170 P. Madhavan, R. Sougrat, A. R. Behzad, K.-V. Peinemann and S. P. Nunes, *J. Membr. Sci.*, 2015, **492**, 568–577.
171 Y. Elhamarnah, H. Qiblawey and M. Nasser, *J. Mol. Liq.*, 2024, **398**, 124250.
172 W. Silva, M. Zanatta, A. S. Ferreira, M. C. Corvo and E. J. Cabrita, *Int. J. Mol. Sci.*, 2020, **21**, 7745.
173 J. Hulsbosch, D. E. De Vos, K. Binnemans and R. Ameloot, *ACS Sustainable Chem. Eng.*, 2016, **4**, 2917–2931.
174 K. Karuppasamy, J. Theerthagiri, D. Vikraman, C.-J. Yim, S. Hussain, R. Sharma, T. Maiyalagan, J. Qin and H.-S. Kim, *Polymers*, 2020, **12**, 918.
175 C. Wang, X. Luo, X. Zhu, G. Cui, D.-e. Jiang, D. Deng, H. Li and S. Dai, *RSC Adv.*, 2013, **3**, 15518–15527.
176 P. Liu, J.-W. Hao, L.-P. Mo and Z.-H. Zhang, *RSC Adv.*, 2015, **5**, 48675–48704.
177 C. Florindo, F. Lima, B. D. Ribeiro and I. M. Marrucho, *Curr. Opin. Green Sustain. Chem.*, 2019, **18**, 31–36.
178 K. Radošević, M. C. Bubalo, V. G. Srček, D. Grgas, T. L. Dragičević and I. R. Redovniković, *Ecotoxicol. Environ. Saf.*, 2015, **112**, 46–53.
179 Y. Zhao, Y. Dong, Y. Guo, F. Huo, F. Yan and H. He, *Chin. J. Chem. Eng.*, 2021, **31**, 113–125.
180 Y. S. Vygodskii, O. A. Mel'nik, E. I. Lozinskaya, A. S. Shaplov, I. A. Malyshkina, N. D. Gavrilova, K. A. Lyssenko, M. Y. Antipin, D. G. Golovanov, A. A. Korlyukov, N. Ignat'ev and U. Welz-Biermann, *Polym. Adv. Technol.*, 2007, **18**, 50–63.
181 G. Q. Lai, F. M. Ma, Z. Q. Hu, H. Y. Qiu, J. X. Jiang, J. R. Wu, L. M. Chen and L. B. Wu, *Chin. Chem. Lett.*, 2007, **18**, 601–604.
182 Z. Ziobrowski and A. Rotkegel, *Maced. J. Chem. Chem. Eng.*, 2020, **39**, 101–108.
183 S. Chen, Y. Dong, J. Sun, P. Gu, J. Wang and S. Zhang, *Green Chem.*, 2023, **25**, 5813–5835.
184 S. N. A. Shafie, N. A. H. Md Nordin, S. M. Racha, M. R. Bilad, M. H. D. Othman, N. Misdan, J. Jaafar, Z. A. Putra and M. D. H. Wirzal, *J. Mol. Liq.*, 2022, **358**, 119192.
185 H. A. Mannan, D. F. Mohshim, H. Mukhtar, T. Murugesan, Z. Man and M. A. Bustam, *J. Ind. Eng. Chem.*, 2017, **54**, 98–106.
186 J. S. Cardoso, Z. Lin, P. Brito and L. M. Gando-Ferreira, *Inorganics*, 2023, **11**, 447.
187 M. M. H. Shah Buddin, A. L. Ahmad and M. A. A. Mohd Saufi, *Asia–Pac. J. Chem. Eng.*, 2023, **18**, e2853.
188 T. Patil, S. Dharaskar, M. k. Sinha, J. Pandya, S. Shinde, S. S. K. Jampa, M. Sillanpaa and C. Yoo, *Int. J. Greenhouse Gas Control*, 2023, **124**, 103856.
189 A. Ghadimi, M. Amirilargani, T. Mohammadi, N. Kasiri and B. Sadatnia, *J. Membr. Sci.*, 2014, **458**, 14–26.
190 I. R. Mazzei, D. Nikolaeva, A. Fuoco, S. Loïs, S. Fantini, M. Monteleone, E. Esposito, S. J. Ashtiani, M. Lanč, O. Vopička, K. Friess, I. F. J. Vankelecom and J. C. Jansen, *Membranes*, 2020, **10**, 224.
191 H. Rabiee, A. Ghadimi and T. Mohammadi, *J. Membr. Sci.*, 2015, **476**, 286–302.
192 K. Zhang, L. Zhou, Z. Wang, H. Li, Y. Yan and J. Zhang, *Phys. Chem. Chem. Phys.*, 2022, **24**, 23690–23698.
193 P. Zhang, Z. Tu, Z. Yan, X. Zhang, X. Hu and Y. Wu, *J. Hazard. Mater.*, 2023, **460**, 132515.
194 Saif-ur-Rehman, M. K. U. Zaman, M. Ahsan Waseem, S. U. Zaman and M. Shozab Mehdi, *Eng. Proc.*, 2021, **12**, 61.
195 Saif-ur-Rehman, M. S. Mehdi, M. Fakhar-e-Alam, M. Asif, J. Rehman, R. A. Alshgari, M. Jamal, S. U. Zaman, M. Umar, S. Rafiq, N. Muhammad, J. Fawad and S. A. Shafiee, *Molecules*, 2023, **28**, 7162.
196 R. Craveiro, L. A. Neves, A. R. C. Duarte and A. Paiva, *Sep. Purif. Technol.*, 2021, **254**, 117593.
197 U. Saeed, A. L. Khan, M. A. Gilani, M. R. Bilad and A. U. Khan, *J. Mol. Liq.*, 2021, **342**, 117509.
198 S. S. Shahabi, N. Azizi and V. Vatanpour, *J. Membr. Sci.*, 2020, **610**, 118267.
199 F. Russo, M. Tiecco, F. Galiano, R. Mancuso, B. Gabriele and A. Figoli, *J. Membr. Sci.*, 2022, **649**, 120387.
200 Y. S. Khoo, T. C. Tjong, J. W. Chew and X. Hu, *Sci. Total Environ.*, 2024, **922**, 171238.

201 X. Liang, J. Zhang, Z. Huang and Y. Guo, *Ind. Crops Prod.*, 2023, **194**, 116351.
202 C. Abels, C. Redepenning, A. Moll, T. Melin and M. Wessling, *J. Membr. Sci.*, 2012, **405–406**, 1–10.
203 S. Cheshmekhezr, S. R. Rothee, M. Nazaripour, A. Rahman, H. Heidari, S. U. Masrura and E. Khan, *npj Mater. Sustain.*, 2024, **2**, 38.
204 B. Adigun, B. P. Thapaliya, H. Luo and S. Dai, *RSC Sustainability*, 2024, **2**, 2768–2780.
205 G. Marco-Velasco, A. Gálvez-Subiela, R. Jiménez-Robles, M. Izquierdo, A. Cháfer and J. D. Badia, *Polymers*, 2024, **16**, 2604.
206 N. Othman, N. F. M. Noah, L. Y. Shu, Z.-Y. Ooi, N. Jusoh, M. Idroas and M. Goto, *Chin. J. Chem. Eng.*, 2017, **25**, 45–52.
207 S. H. Chang, *Desalin. Water Treat.*, 2014, **52**, 88–101.
208 M. B. Rosly, N. Jusoh, N. Othman, H. A. Rahman, N. F. M. Noah and R. N. R. Sulaiman, *Chem. Eng. Res. Des.*, 2019, **145**, 268–278.
209 M. B. Rosly, N. Othman and H. A. Rahman, *Malaysian J. Anal. Sci.*, 2018, **22**, 702–714.
210 A. Kumar, A. Thakur and P. S. Panesar, *Sep. Purif. Technol.*, 2019, **211**, 54–62.
211 A. Kumar, A. Thakur and P. S. Panesar, *J. Cleaner Prod.*, 2018, **181**, 574–583.
212 Purtika, A. Thakur and G. K. Jawa, *Colloids Surf., A*, 2022, **644**, 128776.
213 A. Farhadian, A. Rahimi, N. Safaei, A. Shaabani, E. Sadeh, M. Abdouss and A. Alavi, *ACS Appl. Mater. Interfaces*, 2021, **13**, 3119–3138.
214 M. Usman, S. Cheng, S. Boonyubol and J. S. Cross, *Energies*, 2023, **16**, 5852.
215 *Intensification of Liquid–Liquid Processes*, ed. L. R. Weatherley, Cambridge University Press, Cambridge, 2020, pp. 130–166, DOI: **10.1017/9781108355865.004**.
216 P. Daraei, A. Shokri and E. Rostami, *J. Membr. Sci. Technol.*, 2022, **8**, 526001.
217 K. Anarakdim, M. Matos, A. Cambiella, O. Senhadji-Kebiche and G. Gutiérrez, *Chem. Eng. Process.: Process Intensif.*, 2020, **158**, 108178.
218 K. Anarakdim, M. Matos, O. Senhadji-Kebiche and M. Benamor, *Desalin. Water Treat.*, 2017, **72**, 281–289.
219 P. Davoodi-Nasab, A. Rahbar-Kelishami and M. Raji-Asadabadi, *Desalin. Water Treat.*, 2017, **80**, 234–246.
220 S. Zereshki, A. Shokri and A. Karimi, *J. Mol. Liq.*, 2021, **325**, 115251.
221 V. Kumar, R. K. Singh and P. Chowdhury, *J. Ind. Eng. Chem.*, 2018, **67**, 109–122.
222 S. Gupta, A. Yadav and N. Verma, *Chem. Eng. J.*, 2017, **307**, 729–738.
223 F. V. Hackbarth, D. Maass, A. A. Ulson de Souza, V. J. P. Vilar and S. M. A. Guelli Ulson de Souza, *Chem. Eng. J.*, 2016, **290**, 477–489.
224 D. Kavitha, S. Baral and S. Ganesan, *Chem. Eng. Technol.*, 2023, **46**, 934–939.
225 R. N. R. Sulaiman, N. Othman, N. H. Harith, H. A. Rahman, N. Jusoh, N. F. M. Noah and M. B. Rosly, *Chem. Eng. Commun.*, 2021, **208**, 483–499.
226 H. Wen, S. Nan, D. Wu, Q. Sun, Y. Tong, J. Zhang, S. Jin and W. Shen, *Ind. Eng. Chem. Res.*, 2023, **62**, 20473–20491.
227 Y. Wang, Y. Li, Z. Tang, H. Li, Z. Yuan, H. Tao, N. Zou, T. Bao, X. Liang, Z. Chen, S. Xu, C. Bian, Z. Xu, C. Wang, C. Si, W. Duan and Y. Xu, *Sci. Bull.*, 2024, **69**, 2514–2521.
228 G. Ignacz, N. Alqadhi and G. Szekely, *Adv. Membr.*, 2023, **3**, 100061.
229 M. Jafari, C. Tzirtzipi and B. Castro-Dominguez, *J. Water Process. Eng.*, 2024, **68**, 106532.
230 Z. Cao, O. Barati Farimani, J. Ock and A. Barati Farimani, *Nano Lett.*, 2024, **24**, 2953–2960.
231 A. Chandrasekaran, C. Kim, S. Venkatram and R. Ramprasad, *Macromolecules*, 2020, **53**, 4764–4769.
232 B. Sanchez-Lengeling, L. M. Roch, J. D. Perea, S. Langner, C. J. Brabec and A. Aspuru-Guzik, *Adv. Theory Simul.*, 2019, **2**, 1800069.
233 J. Kern, S. Venkatram, M. Banerjee, B. Brettmann and R. Ramprasad, *Phys. Chem. Chem. Phys.*, 2022, **24**, 26547–26555.
234 R. Gómez-Bombarelli, J. Aguilera-Iparraguirre, T. D. Hirzel, D. Duvenaud, D. Maclaurin, M. A. Blood-Forsythe, H. S. Chae, M. Einzinger, D.-G. Ha, T. Wu, G. Markopoulos, S. Jeon, H. Kang, H. Miyazaki, M. Numata, S. Kim, W. Huang, S. I. Hong, M. Baldo, R. P. Adams and A. Aspuru-Guzik, *Nat. Mater.*, 2016, **15**, 1120–1127.
235 C. W. Coley, W. H. Green and K. F. Jensen, *Acc. Chem. Res.*, 2018, **51**, 1281–1289.
236 S. K. Bishnu, S. Y. Alnouri and D. M. Al-Mohannadi, *Digit. Chem. Eng.*, 2023, **8**, 100111.
237 L. Myllyaho, M. Raatikainen, T. Männistö, T. Mikkonen and J. K. Nurminen, *J. Syst. Softw.*, 2021, **181**, 111050.
238 J. Jaafar and A. M. Nasir, *Front. Membr. Sci. Technol.*, 2022, **1**, 883913.
239 Y. Chen and T. Mu, *Green Chem. Eng.*, 2021, **2**, 174–186.
240 C. Wang, H. Luo, D. E. Jiang, H. Li and S. Dai, *Angew. Chem., Int. Ed.*, 2010, **49**, 5978–5981.
241 X. Ge, C. Gu, X. Wang and J. Tu, *J. Mater. Chem. A*, 2017, **5**, 8209–8229.
242 Q. Zhang, K. De Oliveira Vigier, S. Royer and F. Jérôme, *Chem. Soc. Rev.*, 2012, **41**, 7108–7146.

